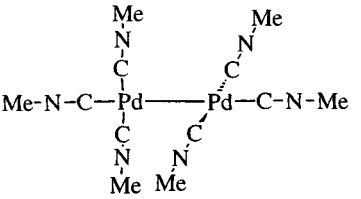

Figure 3.22 The staggered structure of $[Pd_2(MeNC)_6]^{2+}$.

3.8 Complexes of palladium(II) and platinum(II)

A wide variety of complexes are formed by both metals in the +2 oxidation state; indeed, it is the most important one for palladium. The complexes can be cationic, neutral or anionic. Both Pd^{2+} and Pt^{2+} are 'soft' acids so that many stable complexes are formed with S or P as donor atoms but few with O-donors, though there are important ammines. There are pronounced similarities between corresponding palladium and platinum complexes; the latter are more studied (and less labile).

3.8.1 Complexes of O-donors

Complexes of O-donors are relatively rare, explicable by the 'soft' nature of the divalent ions. A telling indication is that sulphoxide ligands will only bind through O if steric effects make S-bonding impractical. The most important complexes are diketonates and carboxylates (for the aqua ions see section 3.5).

Diketonates
Two kinds of platinum diketonate may be made

$$PtCl_4^{2-} + MeCOCH_2COMe \xrightarrow{KOH} KPtCl(acac)_2$$

$$\xrightarrow[\text{exc. } MeCOCH_2COMe]{KOH} Pt(acac)_2$$

$Pt(acac)_2$ has the expected square planar coordination by oxygen (Pt–O 1.979–2.008 Å) with bidentate diketonates; this has also been confirmed for $Pd(PhCOCHCOMe)_2$, which is obtainable as *cis*- and *trans*-isomers that can be crystallized and separated manually (Figure 3.23).

In $[PtCl(acac)_2]^-$, 4-coordination is possible because one of the diketonates is C-bonded (Figure 3.24).

The diketonates can form Lewis base adducts such as 5-coordinate Pd[P(*o*-tolyl)$_3$]$(CF_3COCHCOCF_3)_2$ (Figure 3.25), though with acetylacetone square planar adducts of the type $M(acac)_2(PR_3)_2$ are usually obtained, where the diketone is monodentate O-bonded [63].

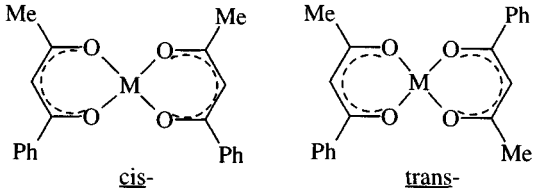

Figure 3.23 The *cis*- and *trans*-isomers of $[Pd(PhCOCHCOMe)_2]$.

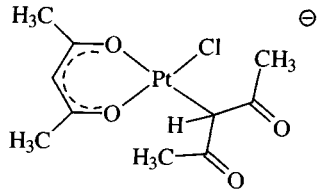

Figure 3.24 The structure of $[PtCl(acac)_2]^-$.

Carboxylates

The acetates are important compounds (Figure 3.26) with somewhat different structures [64], the palladium compound being a trimer (Pd–Pd 3.10–3.20 Å; Pd–O 1.99 Å) while platinum acetate is a tetramer (Pt–O 2.00–2.16 Å; Pt–Pt 2.492–2.498 Å).

There is significant metal–metal bonding in the platinum compound, whose geometry involves a square of platinum atoms; another important difference is that the coordination geometry is square planar in palladium acetate but octahedral in the platinum analogue. Different oligomers exist in solution, broken down by adduct formation. Palladium(II) acetate may be obtained as brown crystals from the following reaction [65]:

$$Pd \xrightarrow[HNO_3]{MeCOOH} Pd(OCOMe)_2$$

The importance of palladium acetate lies in its ability to catalyse a wide range of organic syntheses: functionalizing C–H bonds in alkanes and in aromatics, and in oxidizing alkenes. It has been used industrially in the

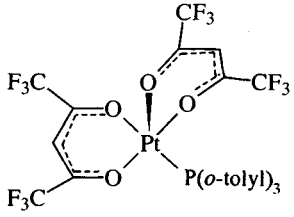

Figure 3.25 The structure of $[Pt(CF_3COCHCOCF_3)_2\{P(o\text{-tolyl})_3\}]$.

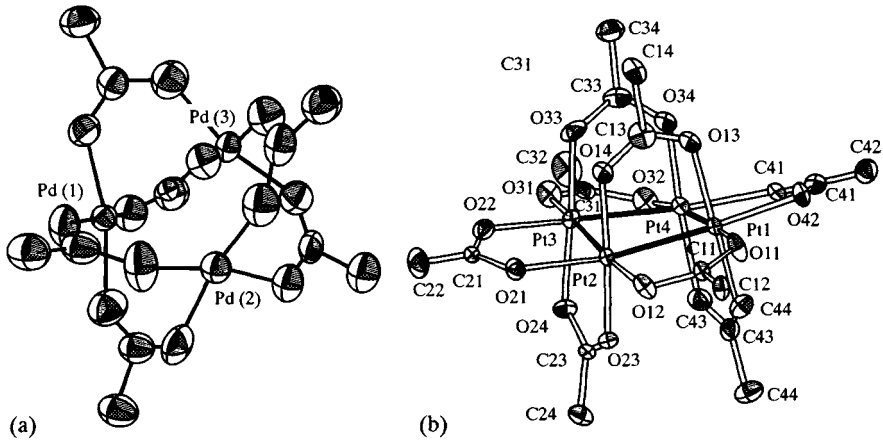

Figure 3.26 The structures of (a) palladium acetate and (b) platinum acetate. (Reproduced with permission from *J. Chem. Soc., Chem. Commun.*, 1970, 659 and *Acta Crystallogr. Sect. B*, 1978, **34**, 1857.)

synthesis of vinyl acetate from ethene; it will also catalyse the conversion of benzene into phenol or benzoic acid. It usually is used in conjunction with a reoxidation catalyst (peroxides, O_2, $K_2S_2O_8$) so that it seems the ability of palladium to switch oxidation states may be important [66],

3.8.2 Complexes of N-donors

Ammines

The preparation of the isomeric forms of $Pt(NH_3)_2Cl_2$ is discussed in terms of the *trans*-effect in section 3.8.9 [67].

$$PtCl_4^{2-} \xrightarrow{\text{aq. } NH_3} \textit{cis}\text{-}Pt(NH_3)_2Cl_2$$

$$Pt(NH_3)_4^{2+} \xrightarrow[\text{heat}]{\text{HCl (aq.)}} \textit{trans}\text{-}Pt(NH_3)_2Cl_2$$

A more convenient synthesis of the latter is

$$Pt(NH_3)_4Cl_2 \xrightarrow[\textit{in vacuo}]{190^\circ C} \textit{trans}\text{-}Pt(NH_3)_2Cl_2 + 2NH_3$$

These *cis*-complexes of palladium are unstable and rapidly isomerize but can be made via the *cis*-diaqua complex [68]

$$Pd(NH_3)_4^{2+} \xrightarrow[HClO_4]{H_2O} \textit{cis}\text{-}Pd(NH_3)_2(H_2O)_2^{2+}$$

$$\xrightarrow[(X=Cl,Br,I)]{NaX} \textit{cis}\text{-}Pd(NH_3)_2X_2$$

$$Pd(NH_3)_4Cl_2 \xrightarrow{H^+} \textit{trans}\text{-}Pd(NH_3)_2Cl_2$$

Although the bisammine complexes of platinum(II) are the most important because of the medical applications of the *cis*-isomer (section 3.10), the synthesis of the others [69] is also important:

$$PtCl_6^{2-} \xrightarrow[HCl]{SO_2} H_2PtCl_4 \xrightarrow[heat]{\text{conc. } NH_3} [Pt(NH_3)_4]Cl_2$$

Pt–N distances are 2.046–2.047 Å in the methane sulphonate salt of $[Pt(NH_3)_4]^{2+}$ [63].

High yield synthesis of $Pt(NH_3)_3Cl^+$ is difficult [67]: the traditional method of Chugaev (*J. Chem. Soc.*, 1915, 1247), which relies on the hydrolysis of NCO^- to generate ammonia, is the most widely used

$$cis\text{-}Pt(NH_3)_2Cl_2 \xrightarrow[heat]{KNCO} Pt(NH_3)_3Cl^+$$

Another route ultimately relies on replacement of a labile water molecule:

$$trans\text{-}Pt(NH_3)_2Cl_2 \xrightarrow[24\,h]{KI} trans\text{-}Pt(NH_3)_2ClI \xrightarrow[boil]{AgNO_3}$$

$$trans\text{-}[Pt(NH_3)_2Cl(H_2O)]^+NO_3^- \xrightarrow[heat]{NH_3} [Pt(NH_3)_3Cl]Cl$$

For the monoammine [67, 70]

$$cis\text{-}Pt(NH_3)_2Cl_2 \xrightarrow{CH_3COOH/KCl} Pt(NH_3)Cl_3^-$$

$$\xrightarrow{Pt(NH_3)_4^{2+}} Pt(NH_3)_4[Pt(NH_3)Cl_3]_2$$

$$\xrightarrow{K_2PtCl_4} KPt(NH_3)Cl_3$$

More conveniently

$$cis\text{-}Pt(NH_3)_2Cl_2 \xrightarrow[MeCONMe_2\ 100°C,\ 6\,h]{Et_4NCl/N_2} Pt(NH_3)Cl_3^-$$

Replacement of the chlorines in *cis*-$Pt(NH_3)_2Cl_2$ is facile (Figure 3.27).

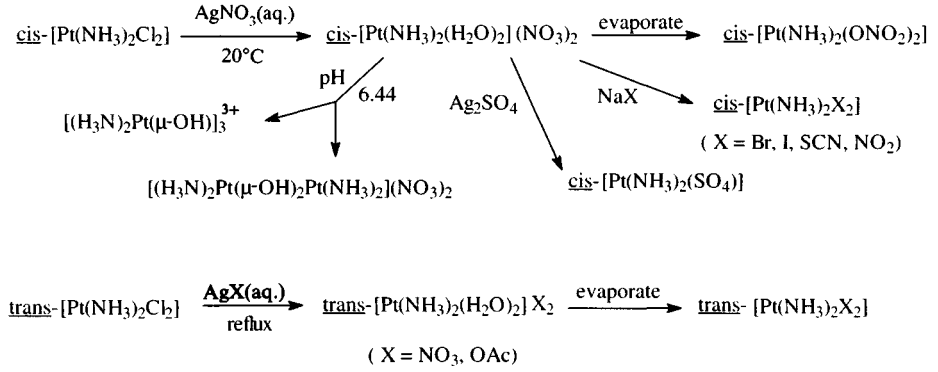

Figure 3.27 Reactions of *cis*- and *trans*-$[Pt(NH_3)_2Cl_2]$.

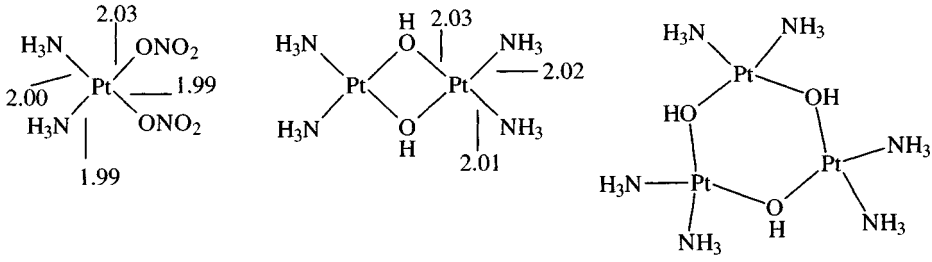

Figure 3.28 Structures of platinum ammine complexes.

It is believed that this occurs when cisplatin is used as an anti-cancer agent. In cells where chloride levels are low, after cisplatin has been transported through the cell wall, the aqua complex (from which other *cis*-complexes are easily made) is formed and is the real anti-cancer agent. At higher pH (~6.5) oligomerization occurs, giving a colourless di-μ-hydroxo bridged dimer and a yellow tri-μ-hydroxo bridged trimer (Figure 3.28) [71, 72].

Kurnakov's test (1893) is generally applicable to *cis*- and *trans*-ammine dihalides. Addition of thiourea (tu, $(H_2N)_2CS$) to the *cis*-complex leads to successive replacement of all the ligands (Figure 3.29); here the lability of the Pt–Cl bond (see section 3.8.9) causes substitution of a chloride.

Since thiourea has a high *trans*-influence, the ammonia *trans* to it is replaced, repetition of the sequence causing the formation of yellow needles of $Pt(tu)_4Cl_2$.

In the case of the *trans*-complex, only the two chloride ions are substituted, the *trans*-effect of ammonia being too low to give substitution with the result that white needle crystals of *trans*-$[Pt(NH_3)_2(tu)_2]Cl_2$ are formed [73].

Another example of reactivity difference lies in the reaction with silver nitrate. Solutions of the *cis*-isomer react with silver nitrate in a few hours at room temperature while the *trans*-isomer needs refluxing for many hours to remove all the chloride [71, 72, 74]. A quantitative method for measuring concentrations of each isomer in mixtures involves reaction

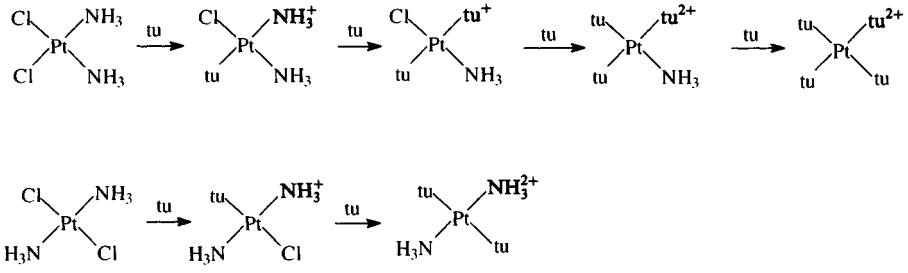

Figure 3.29 Substitution of *cis*- and *trans*-$[Pt(NH_3)_2Cl_2]$ by thiourea (tu) in Kurnakov's test.

with allyl alcohol, which quickly forms a complex $Pt(NH_3)_2Cl(allylalcohol)^+$ with the *trans*-isomer (but not the *cis*-isomer); this can be monitored spectrophotometrically at 252 nm [75].

Distinguishing between cis- and trans-$Pt(NH_3)_2Cl_2$

The relatively recent discovery that *cis*-$Pt(NH_3)_2Cl_2$ possesses significant anti-tumour activity while the *trans*-isomer is inactive has made distinguishing the isomers of greater importance.

Traditionally, the distinction could be achieved by chemical reactions, notably Kurnakov's test, above; the increased scope of physical methods means that several physical techniques can be used in addition to X-ray diffraction studies [76].

Release of coordinated chloride from *trans*-$Pt(NH_3)_2Cl_2$ is much harder and requires heating; *trans*-$PtCl(OH)(NH_3)_2$ (Pt–O 1.989 Å; Pt–N 2.024 and 2.048 Å) and *trans*-$Pt(OH)_2(NH_3)_2$ have been isolated from such mixtures [72].

Among physical methods, dipole moments will distinguish between the two; the *cis*-isomer has a dipole moment while in the *trans*-isomer the bond dipoles cancel. Mixtures of the isomers can be separated chromatographically at low pH [77]. The *cis*- and *trans*-isomers have significantly different vibrational spectra, the PtN_2Cl_2 chromophores approximating to D_{2h} (*cis*) and C_{2v} (*trans*) symmetry, respectively. The *cis*-isomer should give two peaks in the Pt–Cl stretching region of the far-IR spectrum, whereas in the *trans*-isomer only one of the two Pt–Cl stretching vibrations is IR active. Comparison of the far-IR spectra of *cis*-$Pt(NH_3)_2X_2$ (X = Cl, Br) identifies the broad band at 320 cm^{-1}, composed of two overlapping bands, as owing to Pt–Cl stretching. In comparison there is one sharp band in the spectrum of the *trans*-isomer (Figure 3.30) [78]. Raman spectra can similarly be used.

NMR can be used in more than one way [74]. Both isomers will give only one peak in the ^{15}N NMR spectrum, with satellites owing to ^{15}N–^{195}Pt coupling. The coupling constant will depend on the atom *trans* to N; for the *cis*-isomer (N *trans* to Cl) J(Pt–N) is 303 Hz while in the *trans*-isomer (N *trans* to N) it is 278 Hz. The ^{195}Pt spectrum will in each case be a 1 : 2 : 1 triplet owing to coupling of Pt with two equivalent nitrogens (though the value of J varies). The ^{195}Pt chemical shifts are virtually identical.

NQR spectra of the two isomers give resonances at different frequencies and also show that the Pt–Cl bond is more ionic in the *cis*-isomer, while there are significant differences in both the absorption and MCD spectra [79].

Apart from *cis*- and *trans*-$Pt(NH_3)_2Cl_2$, a third compound of this composition can be obtained; unlike the others, it is a 1 : 1 electrolyte:

$$\underset{\text{colourless}}{Pt(NH_3)_4^{2+}(aq.)} + \underset{\text{red}}{PtCl_4^{2-}(aq.)} \rightarrow \underset{\text{green}}{[Pt(NH_3)_4]^{2+}[PtCl_4^{2-}]}$$

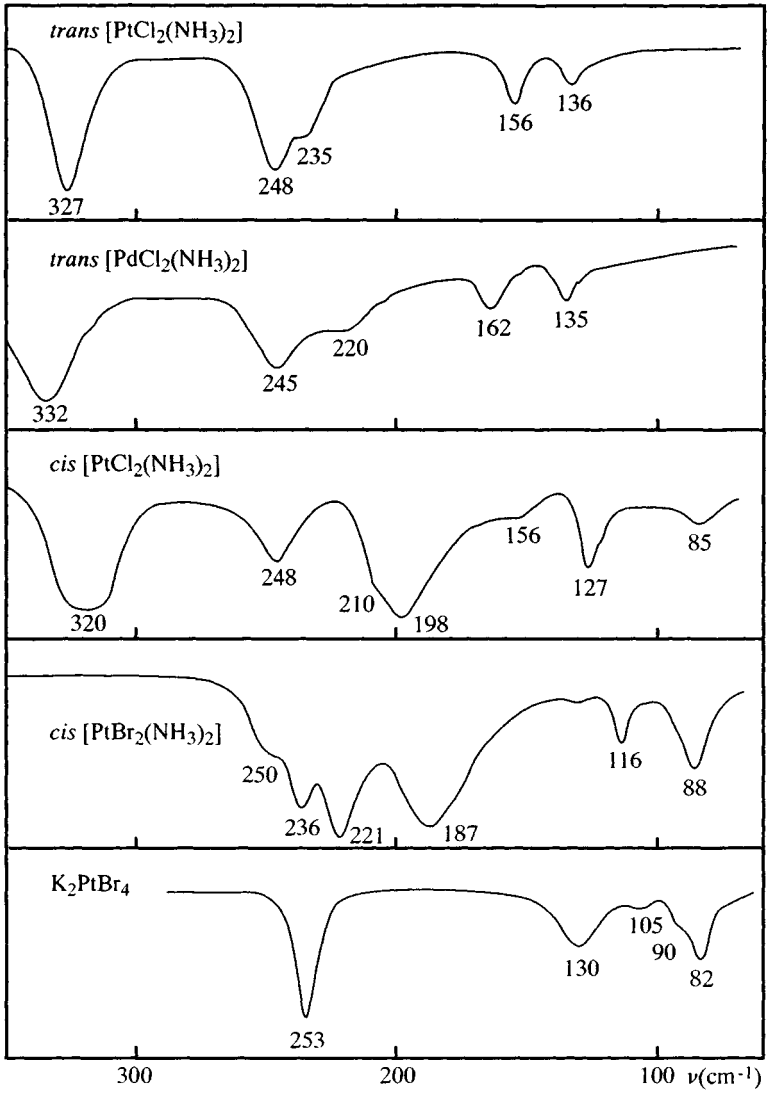

Figure 3.30 IR spectra of *trans*-$[M(NH_3)_2Cl_2]$ (M = Pd, Pt), *cis*-$[Pt(NH_3)_2X_2]$ (X = Cl, Br) and K_2PtBr_4. (Reproduced with permission from *Spectrochim. Acta, Part A*, 1968, **24**, 819.)

The crystal structure (Figure 3.31) shows the cations and anions to be stacked alternately [80] with a Pt–Pt separation of 3.25 Å.

The metal–metal interaction and conductivity increase with pressure; using bulkier ammines increases the Pt–Pt distance. Although palladium-containing ions can be substituted for the platinum species, the optical properties and metal–metal interaction causing pronounced dichroism are

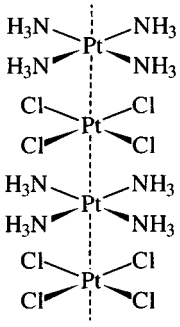

Figure 3.31 Chain structure of $[Pt(NH_3)_4][PtCl_4]$.

associated with the presence of platinum. The Pt–Pt distance is not short enough for metallic conductivity, unlike in the cyanides (section 3.8.4).

On boiling the Magnus salt with ammonia solution, it is converted into the tetraammine

$$Pt(NH_3)_4PtCl_4 + 4NH_3 \rightarrow 2Pt(NH_3)_4Cl_2$$

Magnus' green salt takes its name from its discoverer (1828), H.G. Magnus, Professor of Physics and Technology at the University of Berlin. Pink $[Pd(NH_3)_4]PdCl_4$, Vauqelin's salt, was discovered slightly earlier (1813) by L.-N. Vauquelin, Professor of Chemistry at the Collège de France.

The *cis*- and *trans*-isomers of $Ptpy_2X_2$ can be made by various routes, for example that shown in Figure 3.32.

This synthesis is of course analogous to those for the bisammine complexes. It can be applied to substituted pyridines and other halides (Br, I, NCS) [81].

A recent convenient synthesis for *cis*- and *trans*-$PtpyI_2$ proceeds as follows

$$PtCl_4^{2-} \xrightarrow[KI]{\text{exc.}} PtI_4^{2-} \xrightarrow{py} \textit{cis}\text{-}Ptpy_2I_2$$

This *cis*-isomer is dissolved in DMSO; the initial substitution product is *cis*-$[Ptpy_2(DMSO)I]^+$, which undergoes rapid substitution by iodide to give *trans*-$Ptpy(DMSO)I_2$. Addition of a slight excess of pyridine now gives *trans*-$Ptpy_2I_2$ [82].

It has recently been shown that ^1H NMR spectra can distinguish between *cis*- and *trans*-isomers of this type. The $^3J(Pt–H)$ coupling constants between platinum and the α-hydrogen of the pyridines are slightly higher for the *cis*-isomers; therefore for *cis*-$Ptpy_2Cl_2$ $^3J(Pt–H)$ is 42 Hz while $^3J(Pt–H)$ is 34 Hz for the *trans*-isomer [83].

$$K_2PtCl_4 \xrightarrow[H_2O]{py} \underline{cis}\text{-}Ptpy_2Cl_2 \xrightarrow[heat]{\text{neat py}} [Ptpy_4]Cl_2 \xrightarrow[heat]{\text{conc.HCl}} \underline{trans}\text{-}Ptpy_2Cl_2$$

Figure 3.32 Synthesis of *cis*- and *trans*-$Ptpy_2Cl_2$.

Nitrile complexes $M(RCN)_2Cl_2$ [84] are useful starting materials for the synthesis of other complexes (e.g. phosphine complexes section 3.8.3) as the nitrites are easily displaced. Synthesis include

$$K_2PCl_4 \xrightarrow[25°C,\,8d]{\text{exc. MeCN}} \textit{cis}\text{- and } \textit{trans}\text{-}Pt(MeCN)_2Cl_2$$

$$PtCl_2 \xrightarrow[\text{heat}]{\text{PhCN}} \textit{cis}\text{- and } \textit{trans}\text{-}Pt(PhCN)_2Cl_2$$

Mixtures may be separated by chromatography or by using solubility differences. Isomerization often occurs on heating; solutions of *cis*-$Pt(RCN)_2Cl_2$ give mixtures of the *cis*- and *trans*-forms, while solid *cis*-$Pt(PhCN)_2Cl_2$ gives the *trans*-isomer.

Multidentate amines form many complexes with these metals.

$$K_2MCl_4 \xrightarrow[EtOH/H_2O]{\text{phen}} M(phen)Cl_2$$

$$K_2PtCl_4 \xrightarrow[\text{reflux, 20 h}]{\text{terpy}/H_2O} [Pt(terpy)Cl]^+Cl^-$$

Examples confirmed by X-ray diffraction, all square planar, include *cis*-$Pt(en)Cl_2$ (Pt–N 2.032, Pt–Cl 2.318 Å), *cis*-$Pd(en)Cl_2$ (Pd–N 1.978 Å), $Pd(en)_2Cl_2$ (Pd–N 2.036 Å) [85] and $Pd(bipy)_2(PF_6)_2$ (Pd–N 2.032–2.039 Å). Adoption of a strictly square planar geometry in the last compound would give rise to non-bonded interactions between hydrogens on opposite rings, so that a slight distortion towards a tetrahedral geometry takes place to accommodate this (dihedral angle of 24.1°). In other cases $[Pd(L{-}L)_2](PF_6)_2$ (L–L = bipy, phen), strain is minimized by bowing of the chelating ligands and by the cation assuming a step conformation [86]. Distortion is even more marked in complexes of 2,9-dimethyl-1,10-phenanthroline (diaphen), PtX_2(dimphen) (X = Cl, Br, I), their structures showing the increase in Pt–N bond length as the *trans*-influence of the halogen increases (Table 3.10).

They form adducts with Lewis bases in which the phenanthroline is monodentate, PtX_2(dimphen)L (L = Me_2S, Me_2SO, PhNO) [87].

cis-$Pt(bipy)Cl_2$ exists in yellow and red forms, the difference in colour results from different stacking modes in the solid state, with respective Pt–Pt distances of 4.435 and 3.45 Å [88].

Table 3.10 Distortion of geometry in PtX_2 (dimphen)

X	Pt–N (Å)	Pt–X (Å)
Cl	2.045, 2.046	2.301, 2.313
Br	2.049, 2.058	2.419, 2.421
I	2.062, 2.082	2.580, 2.584

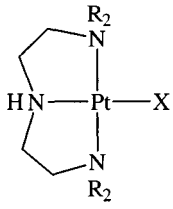

Figure 3.33 The structure of complexes of tridentate amines such as diethylenetriamine.

With tridentate amines like diethylenetriamine (dien) and its relatives, 4-coordination is again the rule, as with $[Pt(dien)Br]^+Br^-$ (Figure 3.33; R = H, X = Br) and $[Pt(Et_4dien)I]^+I^-$ (R = Et, X = I).

The steric crowding introduced in the latter by the four ethyl substituents inhibits nucleophilic attack at platinum, so that complexes of this type tend to undergo substitution by a dissociative mechanism [89]. The complex of the more rigid ligand, 2,2′,2″-terpyridyl, $Pt(terpy)Cl^+$, is found to be about 10^3 to 10^4 times more reactive to substitution than the dien analogue; this is ascribed to steric strain [90], which is reflected in the short Pt–N bond to the 'central' nitrogen (Pt–N some 0.03 Å shorter than the other two Pt–N bonds) and N–Pt–N bond angles of 80–82°).

Another rare example of monodentate phenanthroline is provided by $PtCl(PEt_3)_2(phen)$; the non-bonding Pt–N distance is 2.843 Å (Figure 3.34).

A bidentate phenanthroline would involve considerable non-bonding interactions between the tertiary phosphines and the benzene rings [91].

With their preference for square planar coordination, palladium(II) and platinum(II) are well suited to binding to porphyrins and related N_4 donor macrocycles. Therefore, Pd(octaethylporphyrin) is readily synthesized starting from the labile PhCN complex (like the platinum analogue) [92]

$$MCl_2 + H_2OEP \xrightarrow[195°C,4\,h]{PhCN} 2HCl + M(OEP)$$

It has square planar coordination (Pd–N 2.010–2.017 Å) similar to the value of 2.009 Å in the tetraphenylporphyrin analogue, prepared by a similar route. As with nickel, macrocycle complexes can be made by *in situ* template

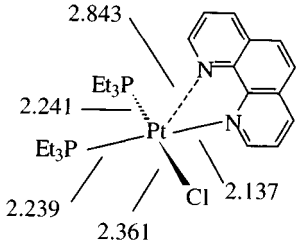

Figure 3.34 The structure of $PtCl(PEt_3)_2(phen)$ showing the monodentate phenanthroline ligand.

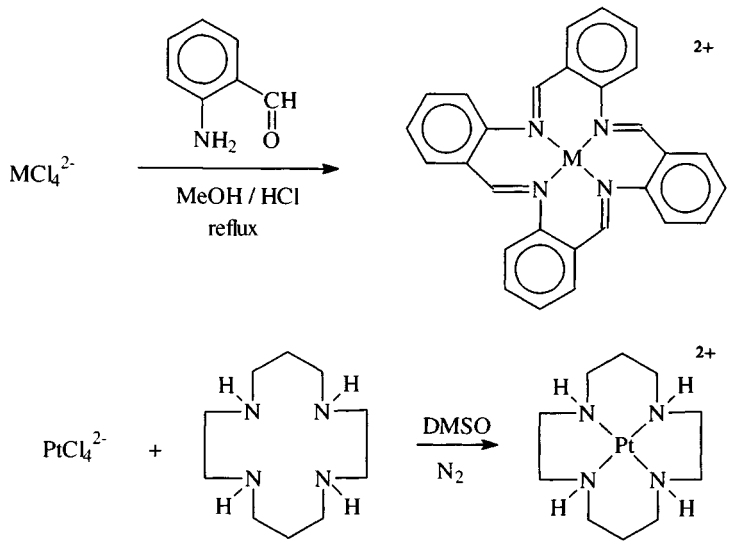

Figure 3.35 Syntheses of complexes of macrocycles.

synthesis (Figure 3.35) using *o*-aminobenzaldehyde [93], or by insertion into a preformed system in the case of the 14aneN$_4$ ligand.

'Platinum blues'

When solutions containing the aqua complexes derived from cisplatin react with pyrimidines and other bases and are exposed to air, blue solutions (and solids) result [94]. These are mixed-valence oligomers ($n = 4$). Some have anti-tumour activity but have not yet found clinical use.

The first structural information was obtained for an α-pyridone complex $[Pt_2(NH_3)_4(pyridone)_2]_2(NO_3)_5$ (Figure 3.36).

It has a chain structure, with one unpaired electron per tetramer unit ($\mu_{eff} = 1.81\,\mu_B$) and can be regarded as a $Pt_3^{II}Pt^{III}$ compound. ESR data suggest that the unpaired electron resides in a MO based on platinum $5d_{z^2}$ orbitals directed along the tetramer chain.

The original 'blue' (K.A. Hofmann, 1908) was obtained from the reaction of $Pt(MeCN)_2Cl_2$ with silver salts over some hours. Under these conditions, the nitrite is hydrolysed to acetamide. Very recently, the structure of the complex $[(H_3N)_2Pt(MeCONH)_2Pt(NH_3)_2]_4(NO_3)_{10}$ has been determined (Figure 3.37).

The average oxidation state of the platinums in the octamer is 2.25.

3.8.3 Tertiary phosphine complexes

Tertiary phosphine complexes of platinum and palladium $M(PR_3)_2X_2$ are important [95]. The *cis*- and *trans*-isomers are readily obtained for platinum,

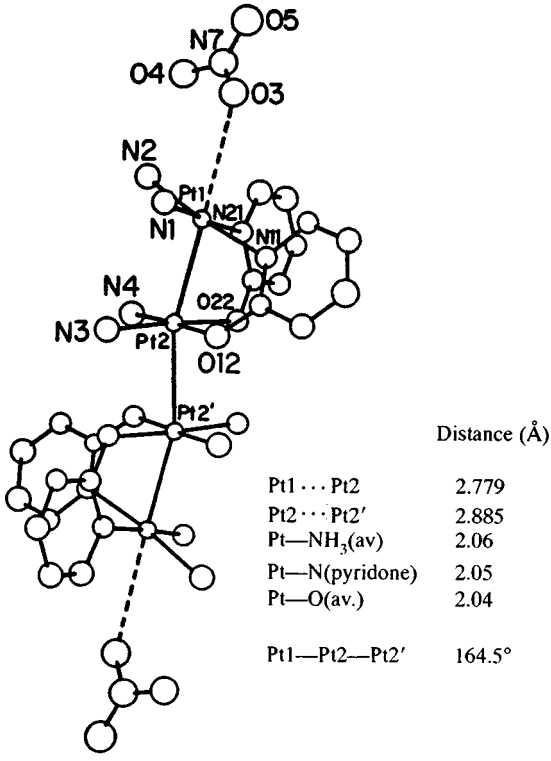

Figure 3.36 Structure of the α-pyridone complex $[Pt_2(NH_3)_4(pyridone)_2]_2(NO_3)_5$. (Reprinted with permission from *J. Am. Chem. Soc.*, 1978, **100**, 3785. Copyright (1978) American Chemical Society.)

but, as found with the ammines (section 3.8.2), *cis*-$Pd(PR_3)_2X_2$ rapidly isomerizes to the *trans*-isomer.

Reaction of K_2PtCl_4 with a trialkyl phosphine initially gives the Magnus-type compound $Pt(PR_3)_4^{2+}PtCl_4^{2-}$. This isomerizes over some weeks (more rapidly on heating) to a mixture of *cis*- and *trans*-$Pt(PR_3)_2Cl_2$, from which the more soluble yellow *trans*-isomer can be extracted with light petroleum, leaving the white *cis*-form to be re-crystallized from ethanol. If the *cis*-form is heated (e.g. in an oil bath) to just above its melting point for around an hour, it will isomerize to the *trans*-isomer.

For the corresponding bromides and iodides, preparation starts with K_2PtX_4 (X = Br, I) formed *in situ* from $PtCl_4^{2-}$ with KX. For *trans*-$Pd(PR_3)_2Cl_2$, shaking alcoholic $PdCl_2$ or Na_2PdCl_4 with the phosphine yields a solution of the yellow complex.

For the triphenylphosphine complexes, where the *cis*-form is particularly stable, irradiation causes the *cis–trans* isomerization

$$K_2PtCl_4 \xrightarrow[\text{reflux}]{PPh_3/\text{xylene}} \textit{cis}\text{-}Pt(PPh_3)_2Cl_2 \xrightarrow[366\,\text{nm}]{h\nu} \textit{trans}\text{-}Pt(PPh_3)_2Cl_2$$

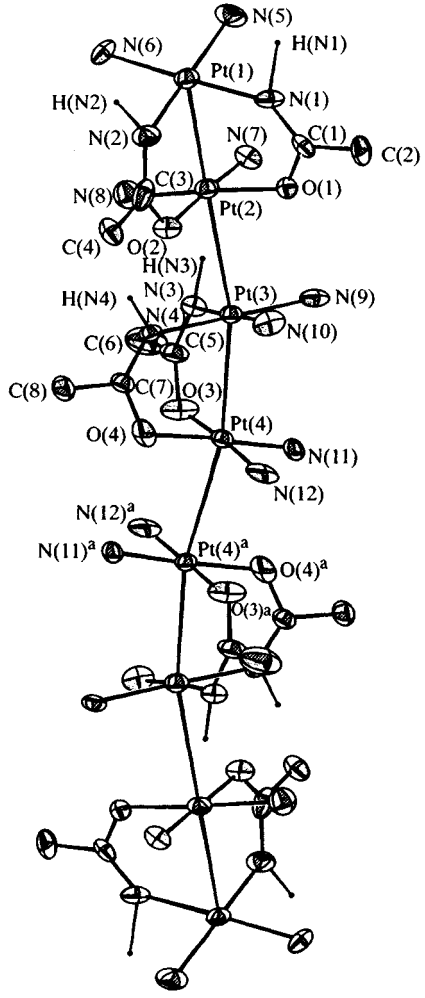

Figure 3.37 Structure of the cation in the acetamide complex $[(NH_3)_2Pt(MeCONH_2)Pt(NH_3)_2]_4(NO_3)_{10}.4H_2O$. (Reprinted with permission from *J. Am. Chem. Soc.*, 1992, **114**, 8110. Copyright (1992) American Chemical Society.)

When halogens add to $Pt(PPh_3)_3$, the initial product is *trans*-$Pt(PPh_3)_2X_2$, isolable after a short reaction time (in the presence of excess X_2, which removes free PPh_3, catalyst for the isomerization to the *cis*-form).

With less bulky phosphines, 5-coordinate $M(PR_3)_3X_2$ can be obtained

$$M(PMe_2Ph)_2X_2 \xrightarrow[CH_2Cl_2]{PMe_2Ph} M(PMe_2Ph)_3X_2$$

$Pd(PMe_2Ph)_3Cl_2$ has a distorted sp structure with a distant axial chlorine (Pd–P 2.265–2.344 Å; Pd–Cl (basal) 2.434 Å; Pd–Cl (axial) 2.956 Å) [96].

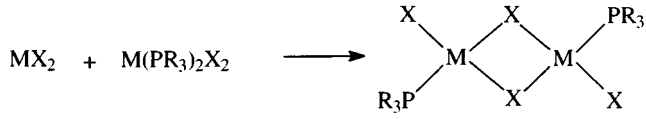

Figure 3.38 Synthesis of the halogen-bridged 1:1 phosphine complexes.

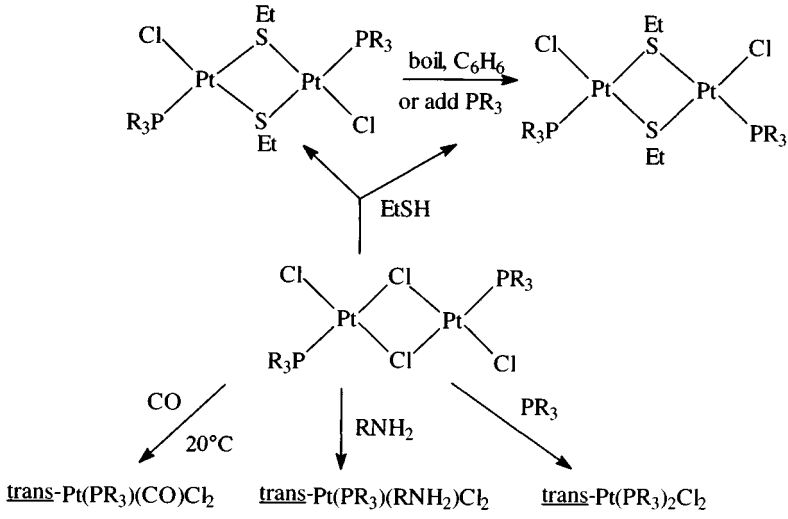

Figure 3.39 Reactions of halogen-bridged 1:1 phosphine complexes.

Halogen-bridged 1:1 complexes can be made by heating together the stoichiometric amounts of MX_2 and $M(PR_3)_2X_2$ in a high boiling solvent (for Pt, naphthalene or xylene: for Pd, ethanol or chloroform) in a reproportionation (Figure 3.38) [97].

Direct synthesis is possible

$$2PtCl_2 + 2PPr^n_3 \xrightarrow{200°C} Pt_2Cl_4(PPr^n_3)_2$$

Various ligands cleave the bridge (Figure 3.39) while thiols substitute at the bridge.

Pfeiffer (1913) pointed out that $[Pt(PR_3)X_2]_2$ complexes can potentially exist in three isomeric forms, but only the symmetric *trans*-isomer has been characterized (Figure 3.40).

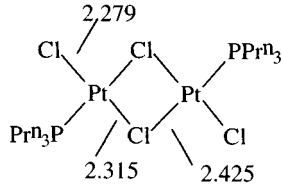

Figure 3.40 The structure of $[Pt(PPr^n_3)Cl_2]_2$.

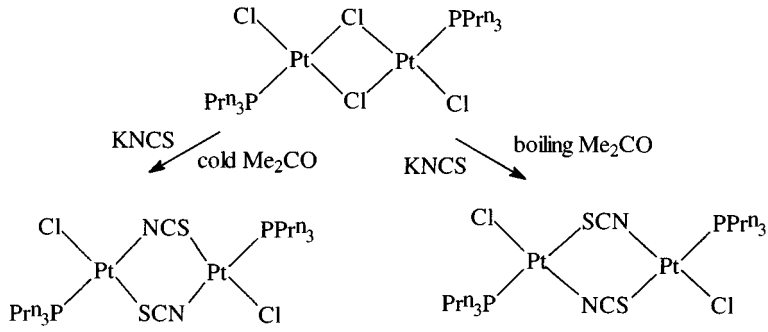

Figure 3.41 Isomerism in bridged thiocyanate complexes.

The greater *trans*-influence of the tertiary phosphine manifests itself in the Pt–Cl bond lengths.

Some interesting cases of isomerism in bridged complexes do arise. The thiocyanate bridged complex shown in Figure 3.41 is a good example of the ambidentate behaviour of the thiocyanate (confirmed by X-ray) while in the complexes $[Pt(PR_3)(SR)(SR')]_2$ the choice of isomer is determined by the order in which the thiolate groups are introduced (Figure 3.42).

Hydride complexes

One and, sometimes, two hydrogen atoms can be introduced into hydride complexes [98]. A variety of synthetic routes has been utilized, using methods

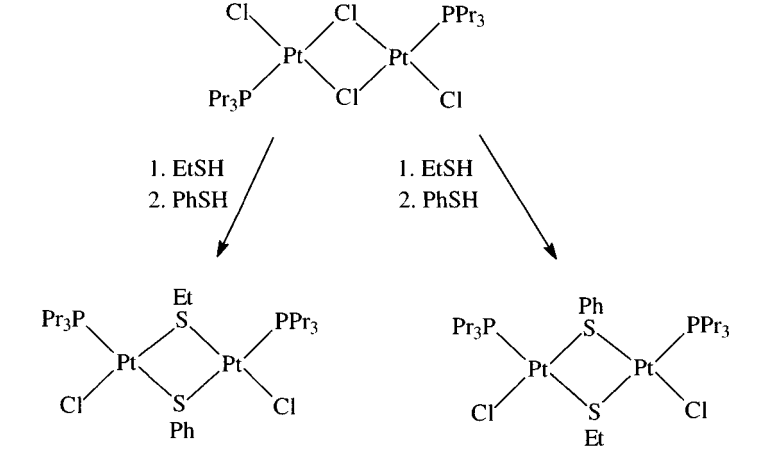

Figure 3.42 Isomerism in bridged thiolate complexes.

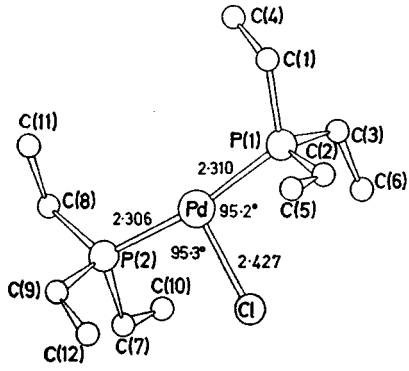

Figure 3.43 The structure of *trans*-$Pd(PEt_3)_2HCl$ (hydride not located). (Reproduced with permission from *J. Chem. Soc., Dalton Trans.*, 1973, 354.)

as diverse as hydrometallate reduction and protonation

$$Pt(PPh_3)_3 \xrightarrow{CF_3CO_2H} [Pt(PPh_3)_3H]^+[(CF_3CO_2)_2H]^-$$

$$\textit{cis}\text{- or } \textit{trans}\text{-}Pt(PEt_3)_2Cl_2 \xrightarrow[\text{heat}]{KOH/EtOH} \textit{trans}\text{-}Pt(PEt_3)_2HCl$$

$$\textit{trans}\text{-}Pd(PEt_3)_2Cl_2 \xrightarrow{Me_3GeH} \textit{trans}\text{-}Pd(PEt_3)_2HCl$$

Some of these monohydrides were among the first transition metal hydride complexes to be synthesized and at the time their geometry was uncertain until X-ray diffraction studies were carried out. The structure of *trans*-$Pd(PEt_3)_2HCl$ shows the geometry to be square planar with the hydrogen exerting stereochemical influence (the hydrogen atom was not located in this study, as hydrogens are poor scatterers of X-rays) (Figure 3.43) [99].

The presence of the hydride group in these complexes can be detected by the observation of ν(M–H) in the IR spectrum (very sensitive to deuteration, by a factor of 0.717 ($\sqrt{\frac{1}{2}}$) (Figure 3.44) and the observation of a low-frequency NMR resonance.

The spectrum of $Pt(PEt_3)_2HCl$ (Figure 3.45) shows a 1:2:1 central resonance owing to coupling of the hydrogen with two equivalent phosphines; the satellites are owing to coupling with ^{195}Pt ($I = 1/2$, 33.8%) [100].

Dihydrides are more difficult to prepare but are most easily obtained with very bulky tertiary phosphines [101a]

$$\textit{trans}\text{-}Pt(PR_3)_2Cl_2 \xrightarrow[EtOH]{\text{exc. } NaBH_4} \textit{trans}\text{-}Pt(PR_3)_2H_2$$

($PR_3 = PBu^t_2$ alkyl, Pcy_3, etc.).

$PtH_2(Pcy_3)_2$ has the IR absorption owing to ν(Pt–H) at 1710 cm^{-1} (a lower frequency than the monohydride owing to the mutually *trans*-hydrogens) and low-frequency NMR line ($\delta = -3.15$ ppm, ^2J(P–H) 17 Hz,

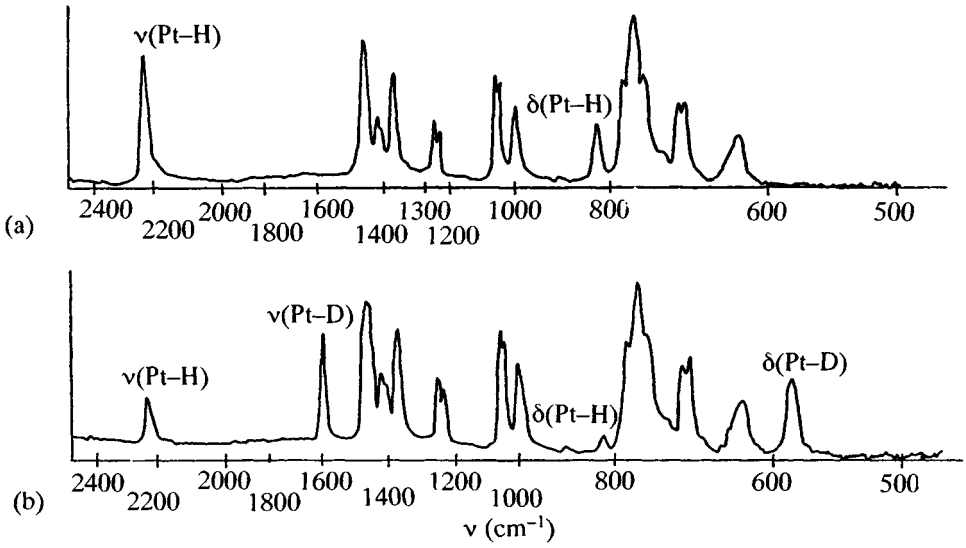

Figure 3.44 IR spectrum of (a) *trans*-$Pt(PEt_3)_2HCl$ and (b) *trans*-$Pt(PEt_3)_2DCl$. (Reproduced with permission from *Proc. Chem. Soc.*, 1962, 321.)

^1J(Pt–H) 790 Hz). The PMe_3 analogue can be prepared by sodium naphthalenide reduction; it is only stable under a hydrogen atmosphere but has, like the Pcy_3 complex, had its structure determined and has the expected spectral properties (IR 1715 cm^{-1}; NMR $\delta = -2.7$ ppm, ^2J(P–H) = 20 Hz, ^1J(Pt–H) 807 Hz). It also exists as the (less stable) *cis*-isomer and is intensely reactive. *trans*-$PtH_2(Pcy_3)_2$ will insert CO_2 to form a formate complex:

$$\textit{trans}\text{-}Pt(Pcy_3)_2H_2 \xrightarrow{CO_2} \textit{trans}\text{-}Pt(Pcy_3)_2H(OCOH)$$

The ion $PtH_3(PBu^t_2)^+_2$ (formed from $PtH_2(PBu^t_3)_2$ and CF_3SO_3H) is believed to be a dihydrogen complex, $[Pt(H)(H_2)(PBu^t_3)_2]^+$ [101b].

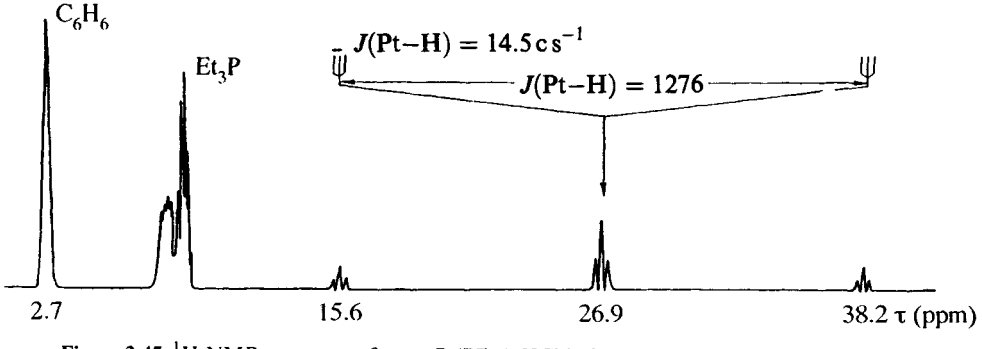

Figure 3.45 ^{1}H NMR spectrum of *trans*-$Pt(PEt_3)_2HCl$ in benzene solution. The τ scale can be converted to the δ scale now used by the relationship $\delta = 10 - \tau$. (Reproduced with permission from *Proc. Chem. Soc.*, 1962, 321.)

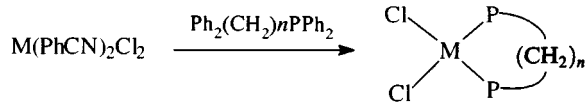

Figure 3.46 Synthesis of 1:1 diphosphine complexes (M = Pd, Pt).

Complexes of bidentate phosphines

Reaction of the diphosphines $Ph_2P(CH_2)_nPPh_2$ ($n = 1$–3) with $MCl_2(PhCN)_2$ affords 1:1 *cis*-complexes (Figure 3.46) [102]. (Note the use of the labile PhCN adducts; if the MCl_4^{2-} salts are used, 'Magnus' type compounds $M(P\text{–}P)_2^{2+}MCl_4^{2-}$ are formed.) Similar complexes are formed with other halides: for the thiocyanates see section 3.8.6. The structures of the palladium complexes have been determined (Table 3.10) with 'square' coordination only achieved for $n = 3$ with the formation of a six-membered metal-chelate ring.

With longer carbon chains in the diphosphine (n, e.g. 5, 6) oligomers are formed, thus $PdCl_2[Ph_2P(CH_2)_6PPh_2]$ is a dimer (Figure 3.47) with Pd–Cl 2.300–2.316 Å, Pd–P 2.342–2.344 Å. (Comparison with the *cis*-complexes in Table 3.10 shows that Pd–P bonds *trans* to P are longer, and Pd–Cl *trans* to Cl are shorter, owing to the *trans*-influence.)

Platinum generally behaves similarly to palladium, though $Pt[Ph_2P(CH_2)_3PPh_2]Cl_2$ is thought to be oligomeric; the monomer $Pt[Ph_2P(CH_2)_5PPh_2]Cl_2$ has a *cis*-structure. It is likely that both monomers and oligomers can be made, depending on choice of reaction conditions and starting materials.

With bulky diphosphines $Bu^t_2P(CH_2)_nPBu^t_2$ ($n = 8$–12), similar reactions of the diphosphines with $MCl_2(PhCN)_2$ give separable mixtures of monomer, dimer and trimer. With small phosphines ($n = 5$–7) dimers predominate (Figure 3.48).

Specific examples where structures have been determined are *trans*-$Pt[Bu^t_2P(CH_2)_{12}PBu^t_2]Cl_2$ and dimeric $[Pd(Bu^t_2P(CH_2)_nPBu^t_2)Cl_2]_2$ ($n = 5$, 7, 10).

The factors determining which complex is obtained are not completely delineated. In a study of a range of $Ph_2P(CH_2)_nPPh_2$ ($n = 2$, 6–12, 16) *cis*-complexes (usually monomer–dimer mixtures) were made from the phosphine and K_2PtCl_4 in refluxing $MeOCH_2CH_2OH$, while using the phosphine

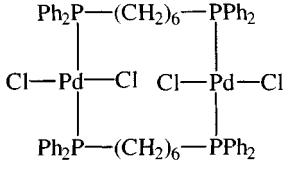

Figure 3.47 The dimeric diphosphine-bridged complex $[Pd\{Ph_2P(CH_2)_6PPh_2\}Cl_2]_2$.

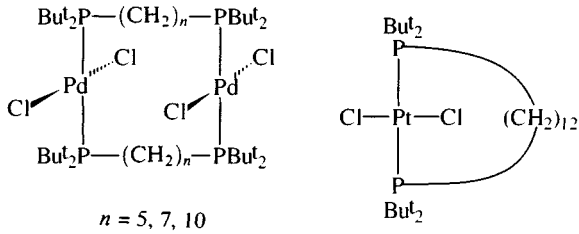

Figure 3.48 The diphosphine complexes $[Pd\{Bu^t_2P(CH_2)_nPBu^t_2\}Cl_2]_2$ and $[Pt\{PBu^t_2P(CH_2)_{12}PPBu^t_2\}Cl_2]$.

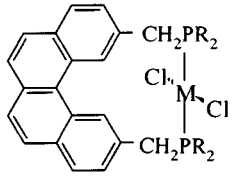

Figure 3.49 The *trans*-complexes of a phenanthrene-derived diphosphine ligand (M = Pd, Pt).

and Zeise's salt in $Me_2CO/CHCl_3$ gave a mixture of monomeric and dimeric *trans*-complexes.

Rigid diphosphines have been used to enforce *trans*-geometries; thus with the phenanthrene-derived diphosphine (Figure 3.49, R = Et) the complexes $PdLCl_2$ and $PtLCl_2$ have closely similar geometries (Pd–P 2.307 Å, Pd–Cl 2.306 Å, P–Pd–P 177.4°; Pt–P 2.293 Å, Pt–Cl 2.304 Å, P–Pt–P 177.1°) [103].

Many, but not all, bidentate phosphine and arsine ligands form 2:1 complexes with these metals. $M(diars)_2X_2$ (diars = o-$C_6H_4(AsMe_3)_2$) contain 6-coordinate metals; *trans*-$Pd(diars)_2I_2$ has long Pd–I bonds (3.52 Å). These complexes are 1:1 electrolytes in solution, suggesting the presence of 5-coordinate $M(diars)_2X^+$ ions.

Complexes of bulky phosphines and internal metallation reactions

The molecular structures of complexes of the platinum metals with tertiary phosphines often show short metal–carbon or metal–hydrogen contacts [104]. When complexes of bulky tertiary phosphines are heated, internal metal–carbon bond formation frequently occurs (Figure 3.50).

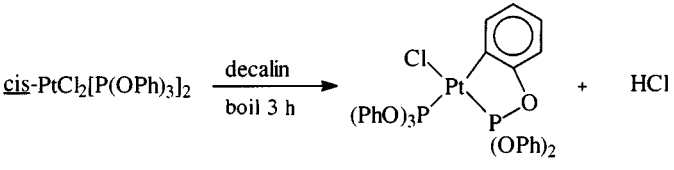

Figure 3.50 Internal metallation of *cis*-$PtCl_2[P(OPh)_3]_2$.

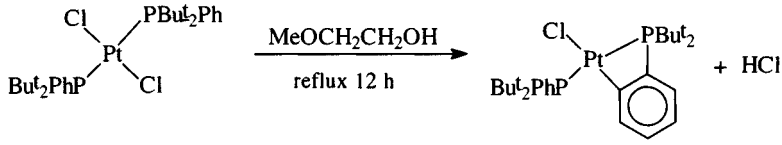

Figure 3.51 Internal metallation of *trans*-$PtCl_2(PBu^t_2Ph)_2$.

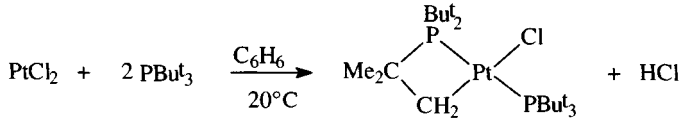

Figure 3.52 Formation of a metallated complex with PBu^t_3 under mild conditions.

This reaction goes less easily with the bromide and not at all with the iodide, nor with any palladium analogue. In another example (Figure 3.51), similar reactions do not occur with less bulky phosphines (PMe_2Ph) and occur less readily with ligands having only one bulky group (e.g. PBu^tPh_2). With the even bulkier PBu^t_3, reflux is not necessary for metallation (Figure 3.52) and there is no evidence for $PtCl_2(PBu^t_3)_2$.

In the case of palladium, *trans*-$PdCl_2(PBu^t_3)_2$ can be isolated, which in solution slowly converts into the internally metallated complex, in keeping with the unwillingness of palladium to metallate. The reason for this may lie in a mechanism involving oxidative addition forming a M(IV) intermediate (Figure 3.53) that then eliminates HCl; the decreased stability of palladium(IV) could make the activation energy for this step too high. Figure 3.54 includes other reactions involving the *t*-butylphosphines showing the effect of steric crowding on metallation.

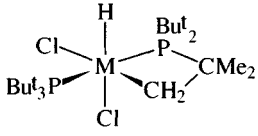

Figure 3.53 Possible M^{IV} intermediate in the formation of a metallated complex with PBu^t_3.

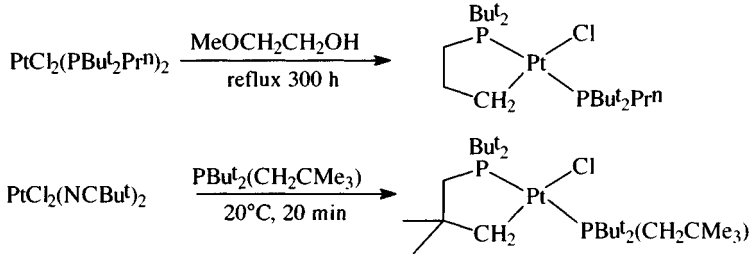

Figure 3.54 The effect of the bulk of tertiary phosphine ligands upon the ease of the formation of a metallated complex.

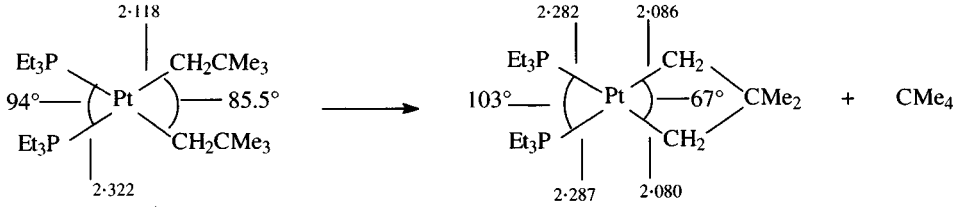

Figure 3.55 Structural evidence for the reduction in strain attending the formation of a metallated complex.

The use of bulky alkyl groups to promote elimination depends on steric crowding; comparison of bond lengths in a bis(neopentyl) and the metallated product (Figure 3.55) shows crowding in the bis(neopentyl) to manifest itself in slight lengthening of the Pt–P bonds (the Pt–C bond is 'normal', see Table 3.11) and a slight twist between the P–Pt–P and C–Pt–C planes (18.7°). The platinacyclobutane product has rather shorter Pt–P and Pt–C bonds.

3.8.4 Complexes of C-donors [105]

Alkyls

Alkyl compounds can be synthesized by substitution, oxidative addition and insertion reactions

$$\textit{trans}\text{-}PtCl_2(PR_3)_2 \xrightarrow{MeMgX} \textit{trans}\text{-}Pt(PR_3)_2MeCl$$

($PR_3 = PMe_2Ph$, PPh_3)

$$Pt(PPh_3)_3 \xrightarrow{MeI} Pt(PPh_3)_2MeI$$

$$\textit{trans}\text{-}Pt(PEt_3)_2HCl + C_2R_4 \rightleftharpoons \textit{trans}\text{-}Pt(PEt_3)_2Cl(CR_2CR_2H) \quad (R = H, F)$$

In the last reaction, use of C_2F_4 drives the equilibrium to the right.

Table 3.11 Bond lengths (Å) in palladium and platinum alkyls and aryls: $M(PR_3)_2R^1X$

	M	PR_3	R^1	X	M–X	M–C	M–P
trans-Isomer	Pt	$PMePh_2$	Me	Cl	2.412	2.081	2.291, 2.292
	Pt	$PMePh_2$	CF_2CF_3	Cl	2.363	2.013	2.326–2.341
	Pt	PMe_2Ph	CH_2SiMe_3	Cl	2.415	2.079	2.292
	Pt	PEt_3	Me	Cl	2.346	2.018	2.293
	Pt	PPh_3	CF_3	Cl	2.400	2.080	2.328
	Pt	PPh_3	Ph	Ph	–	2.080	2.299
cis-Isomer	Pt	$PMePh_2$	Me	Me	–	2.119–2.122	2.284–2.285
	Pd	$PMePh_2$	Me	Me	–	2.089–2.092	2.321–2.326
	Pt	PEt_3	Et	Cl	2.384	2.087	2.210, 2.350

The structures of the series *trans*-$Pt(PMePh_2)_2RCl$ (R = Me, CF_2CF_3) show Pt–C bonds of 2.081 and 2.013 Å, respectively, with the electron-withdrawing fluoroalkyl leading to a shorter and stronger bond. (Data for some other platinum alkyls are discussed in section 3.8.10.)

Palladium alkyls are generally less stable than their platinum analogues. This is not reflected, however, in the molecular dimensions of *cis*-$MMe_2(PMePh_2)_2$: Pt–C 2.120 Å, Pd–C 2.090 Å, Pt–P 2.284, Pd–P 2.323 Å, suggesting that such instability is kinetic rather than thermodynamic in origin [106a]. Planar 4-coordination is general as usual; therefore, in $Pd(C_6F_5)_2$(terpy), the 2,2′:6′,2″-terpyridyl ligand is bidentate [106b].

Reaction of MeLi with $Pt(PPh_3)_2(Me)_2$ gives $Li_2Pt(Me)_4$; $Pt(Me)_4^{2-}$ is of marginal stability in solution. Use of electron-withdrawing groups like C_6Cl_5 confers greater stability; $(Bu_4N)_2[Pt(C_6Cl_5)_4]$ has square planar platinum (Pt–C 2.086 Å). Adduct formation with, for example, tertiary phosphines and arsines can confer considerable stability on alkyls and aryls; thus *cis*-$Pt(PEt_3)_2(Me)_2$ can be distilled at 85°C *in vacuo* (10^{-4} mmHg) without decomposition.

Isomerization and elimination reactions of alkyls and aryls

Isomerizations of mono-alkyls and aryls have been widely studied [107]; many *cis*-$Pt(PR_3)_2ArCl$ undergo rapid isomerization in the presence of free phosphine, a reaction inhibited by Cl^- with a mechanism believed to involve a 3-coordinate $Pt(PR_3)_2Ar^+$ intermediate that is then attacked by Cl^-. The *cis*- and *trans*-isomers of $Pt(PEt_3)_2(Ph)Cl$ undergo reversible isomerization when irradiated at the wavelength of charge-transfer transitions (254 and 280 nm).

Elimination reactions have been particularly studied in the case of dialkyls. They depend on the alkyl groups being *cis*; *trans*-complexes have to isomerize before they can eliminate, and a complex with a *trans*-spanning diphosphine ligand is stable to 100°C (Figure 3.56).

A dissociative mechanism is indicated by the fact that excess phosphine inhibits elimination from molecules like *cis*-$Pd(PPh_3)_2Me_2$ and $Pt(PPh_3)_2Bu_2$. On thermolysis of mixtures where one molecule contains deuterium, such as

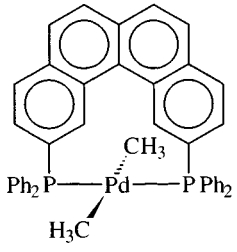

Figure 3.56 A rigid *trans*-dialkyl complex that is particularly stable to thermal elimination.

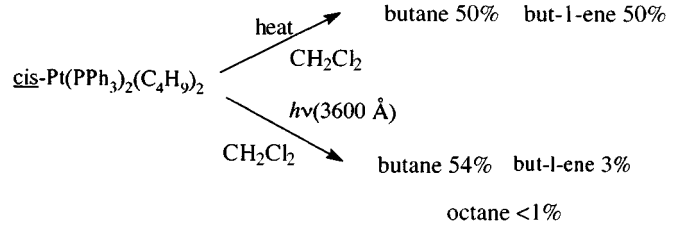

Figure 3.57 The effect of reaction conditions upon decomposition of *cis*-$Pt(PPh_3)_2(C_4H_9)_2$.

cis-$Pd(PR_3)_2Me_2$ and $Pd(PR_3)_2(CD_3)_2$, only C_2H_6 and C_2D_6 were formed, indicating an intramolecular mechanism (similar results were obtained with mixtures of *cis*-$Pt(PPh_3)_2(CH_2CD_2CH_2Me)_2$ and $Pt(PPh_3)_2(C_4H_9)_2$.)

Alkyls with groups that cannot β-eliminate (Me, CH_2SiMe_3) are more stable than those that can (e.g. ethyls). *Trans*-complexes that cannot eliminate by reductive coupling may β-eliminate:

$$\textit{trans}\text{-}Pd(PMe_2Ph)_2Et_2 \xrightarrow{\text{heat}} C_2H_4 + C_2H_6$$

$$\textit{cis}\text{-}Pd(PMe_2Ph)_2Et_2 \xrightarrow{\text{heat}} C_4H_{10}$$

When photolysed, the *cis*- and *trans*-isomers both give ethene, ethane and butane (in a 2:2:1 ratio), the route doubtless involves a photochemical isomerization. If extra PMe_2Ph is added, then dissociative coupling is inhibited, and β-elimination giving C_2H_4 and C_2H_6 is favoured. When *cis*-$Pt(PEt_3)_2Et_2$ is heated to 118°C in solution, β-elimination occurs (yielding C_2H_6 and $Pt(PEt_3)_2(C_2H_4)$) with a mechanism involving phosphine dissociation. Another case where both routes have been examined is shown in Figure 3.57.

The evidence is that the thermolytic route does not involve radicals but the photochemical one does. A dissociative mechanism for the thermolytic route is indicated by its inhibition by added phosphine; it is likely that once a phosphine group has dissociated, a metal–hydrogen bond is formed, with generation of a coordinated alkene (Figure 3.58).

On heating, the neopentyl $Pt(PEt_3)_2(CH_2CMe_3)_2$ undergoes an intramolecular metallation elimination [108a] (Figure 3.59), which appears to involve initial phosphine loss affording a platinum(IV) metallacycle.

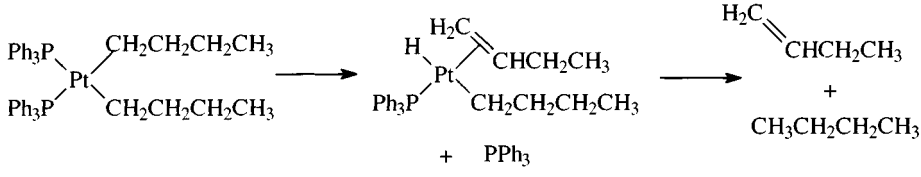

Figure 3.58 A possible mechanism for the thermolytic decomposition of *cis*-$Pt(PPh_3)_2(C_4H_9)_2$.

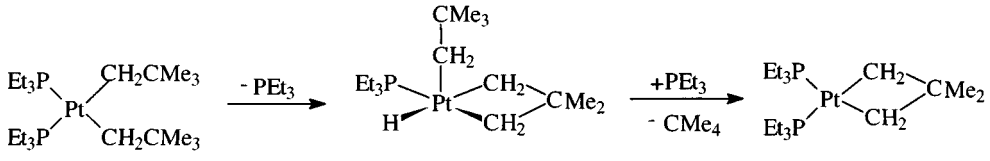

Figure 3.59 A possible mechanism for the thermolytic decomposition of *cis*-$Pt(PEt_3)_2(CH_2CMe_3)_2$.

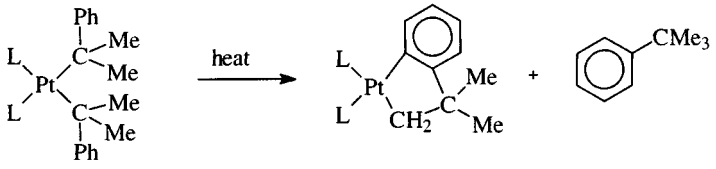

L = PEt_3, PPh_3, ½ phen, ½ bipy, ½ diphos

Figure 3.60 The thermolytic decomposition of $PtL_2(CMe_2Ph)_2$.

Detailed kinetic studies of the decomposition of platinum(II) dineophyls show (Figure 3.60) the exclusive formation of *t*-butylbenzene and an internally metallated platinum complex (3,3-dimethylplatininadan).

The suggested mechanism involves breaking of a platinum–ligand bond, again forming a platinum(IV) hydride that can then eliminate the alkane.

Compounds like *cis*-$[PdMe_2(PR_3)_2]$ (R = Me, Et) have been suggested as chemical vapour deposition (CVD) precursors for palladium [108b].

Platinum (II) carbenes should be mentioned as σ-bonded organometallics. An important general synthesis by cleavage of an electron-rich alkene affords a pair of isomers, the *trans*-form isomerizing to the thermodynamically more stable *cis*-form on heating (Figure 3.61).

The *cis*-isomer has the shorter and stronger Pt–C bond, a reflection of the lower *trans*-influence of chloride [109].

Zeise's salt

Although Zeise's salt is a complex of a π-bonding ligand, this compound must be included in an account of the chemistry of these metals, if only as

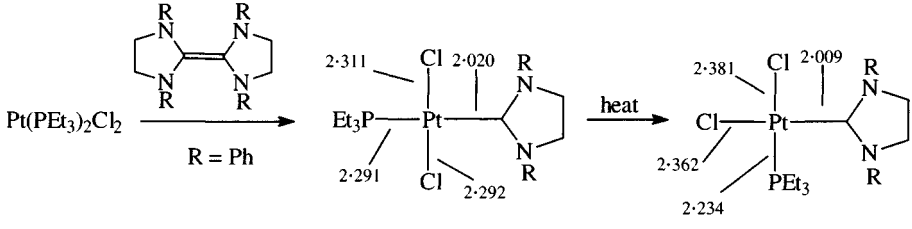

Figure 3.61 The synthesis and structure of two platinum(II) carbenes.

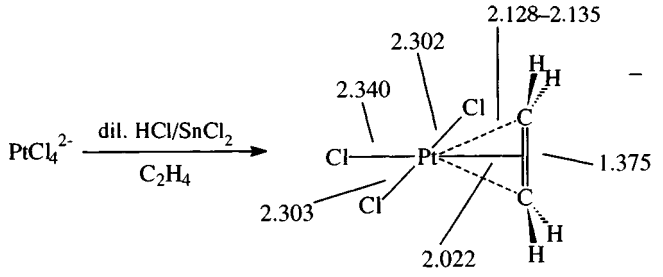

Figure 3.62 Synthesis and structure of Zeise's salt.

the first organometallic to be synthesized (1825) [110a]. It is an important model for the catalytic oxidation of alkenes to aldehydes. Zeise originally obtained it by refluxing an ethanolic mixture of $PtCl_2$ and $PtCl_4$ and extracting the resulting black solid with KCl/HCl. A more convenient method for obtaining yellow crystals of $KPtCl_3(C_2H_4)$ is shown in Figure 3.62, together with its structure.

Features to note in the structure [110b] are:

1. The *trans*-influence of ethene on the Pt–Cl bond
2. At 1.375 Å, the C–C bond in coordinated ethene is some 0.038 Å longer than in free ethene
3. Bending of the four hydrogens away from platinum (the carbons are 0.16 Å out of the plane of the four hydrogens).

Features (2) and (3) are explicable in terms of the Dewar–Chatt–Duncanson model for bonding in alkene complexes (Figure 3.63), which involves

1. Formation of a σ-bond by donation from the π-orbital of ethene into a vacant metal dsp^2 hybrid orbital
2. Back-bonding, with formation of a π-bond, from a filled metal d orbital to an anti-bonding π^*-ethene orbital.

This involves partial occupation of the π^*-orbital and hence a lengthening of the C–C bond; moreover, as the bonding at carbon changes, acquiring some sp^3 character, so the bond angle at carbon will decrease below 120°.

In the Wacker process, the coordinated ethene undergoes nucleophilic attack by OH^-. In the course of the redox reaction, palladium(II) is reduced

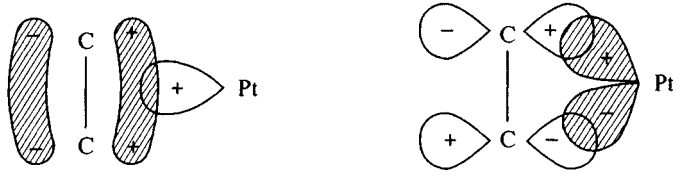

Figure 3.63 Platinum–alkene bonding in Zeise's salt. (Reproduced with permission from S.A. Cotton and F.A. Hart, *The Heavy Transition Elements*, Macmillan Press Ltd, 1975, p. 126.)

to palladium metal but is reoxidized by $CuCl_2/O_2$ *in situ*. In simple form

1. $PdCl_2 + C_2H_4 + H_2O \rightarrow Pd + 2HCl + MeCHO$
2. $Pd + 2CuCl_2 \rightarrow PdCl_2 + 2CuCl$
3. $2CuCl + 2HCl + \frac{1}{2}O_2 \rightarrow 2CuCl_2 + H_2O$

Overall:

$$C_2H_4 + \tfrac{1}{2}O_2 \rightarrow MeCHO$$

Cyanide complexes [111]
Reactions of $PtCl_4^{2-}$ with excess KCN gives yellow $K_2Pt(CN)_4.3H_2O$ (Gmelin, 1822). It contains square planar $Pt(CN)_4^{2-}$ ions stacked parallel (Pt–Pt 3.478 Å) with the groups rotated by 16° relative to the groups above and below (minimizing non-bonding interactions). The palladium analogue $K_2Pd(CN)_4.H_2O$ can be prepared similarly. The C≡N stretching vibrations give rise to strong Raman (2145, 2165 cm^{-1}) and IR (2123 and 2134 cm^{-1}) bands.

The tetracyanometallates exhibit strongly polarized luminescence that can be shifted between the near UV and the near IR (as it is very sensitive to the Pt–Pt distance) by choice of cation and by varying the pressure.

Partial oxidation gives compounds like the bronze 'Krogmann salts', anion deficient $K_2Pt(CN)_4Br_{0.3}.3H_2O$ (Pt–Pt 2.88 Å) or the cation deficient $K_{1.75}Pt(CN)_4.1.5H_2O$ (Pt–Pt 2.96 Å). These compounds are, because of the short Pt–Pt distances, one-dimensional metallic conductors. This is thought to arise through Ptd_{z^2} (or $d_{z^2}-p_z$) orbitals overlapping along the axes of the 'stacked' $Pt(CN)_4$ units (Figure 3.64) [112].

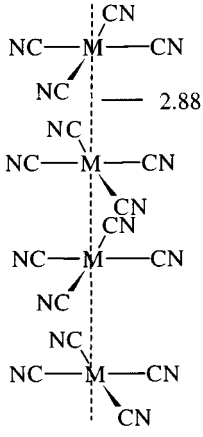

Figure 3.64 The stacking of anions in $K_2Pt(CN)_4Br_{0.3}.3H_2O$.

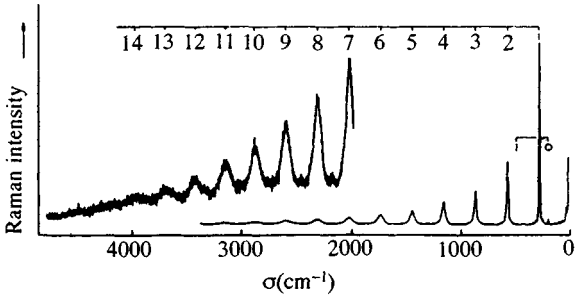

Figure 3.65 Resonance Raman spectra of $[Pt(en)_2][Pt(en)_2Cl_2]_3[CuCl_4]_4$ in a KCl disk at 80 K, $\lambda = 568.2$ nm. (Reproduced with permission from *J. Chem. Soc., Dalton Trans.*, 1980, 2492.)

Other one-dimensional chain compounds [112]

The compound $Pt(EtNH_2)_4Cl_3.H_2O$, Wolffram's red salt, is in fact a mixed-valence compound with alternating square planar $Pt^{II}(EtNH_2)_4^{2+}$ and octahedral $Pt^{IV}(EtNH_2)_4Cl_2^{2+}$ units. This is a prototype for a large number of related compounds with mono-, bi- and multidentate ligands. They have intense colours owing to intervalence charge-transfer transitions polarized along the chain (moving to shorter wavelengths as the halide changes from chloride to iodide and as the platinum–halide bridge shortens; the conductivity similarly increases). These dichroic compounds also exhibit strong resonance Raman spectra with vibrational progressions of the symmetric $X-Pt^{IV}-X$ stretching mode (Figure 3.65) [113].

^{15}N solid-state NMR studies on complexes like $[Pt(en)X_2][Pt(en)X_4]$ (X = halogen) (Figure 3.66) show that not only can separate ^{15}N environments be discerned for the Pt^{II} and Pt^{IV} sites, but the platinum environments become more similar as the halogen becomes less electronegative, the halogen becoming more centrally placed in the chain leading to higher chain conductivity [114].

3.8.5 Complexes of S-donors

Reactions of RSH with MCl_4^{2-} in aqueous solution lead to precipitates of the neutral thiolates $M(SR)_2$; with small alkyl and aryl substituents, the products are oligomeric: $Pd(SPr^i)_2$ is hexameric with square planar palladium (Figure 3.67) [115].

Reactions in acetonitrite lead to anionic thiolates

$$Pd(NO_3)_2 \xrightarrow[MeCN]{1.\ NaSPh \quad 2.\ Ph_4PBr} (Ph_4P)_2Pd_2(SPh)_6$$

$$PtCl_4^{2-} \xrightarrow[MeCN/Me_2CO]{1.\ NaSPh \quad 2.\ Et_4NBr} (Et_4N)_2Pt(SPh)_4$$

The platinum complex is square planar, while the palladium dimer also has planar 4-coordination (for other examples of mercaptide bridges see section 3.8.3) [116].

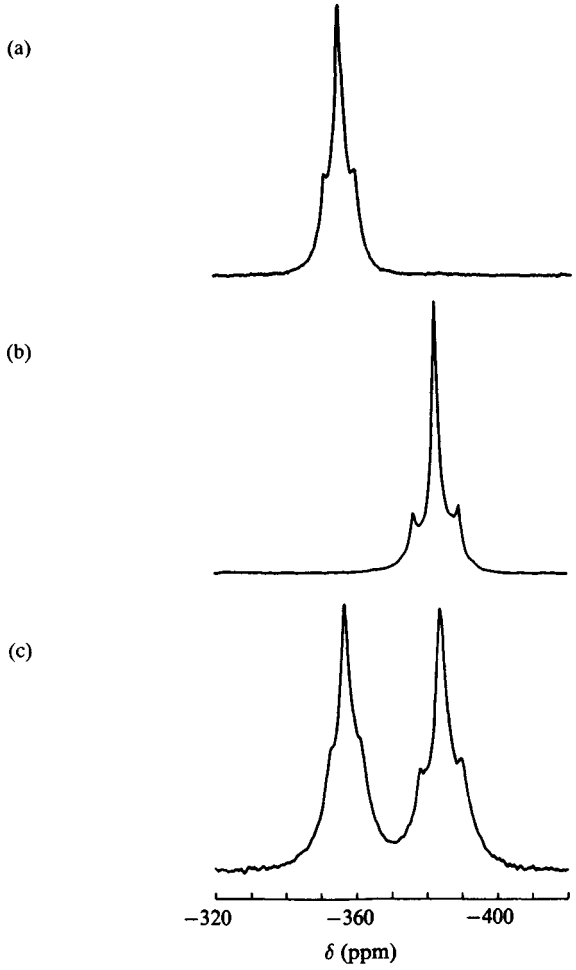

Figure 3.66 Enriched ^{15}N solid-state NMR spectra of (a) $[Pt(en)Cl_4]$; (b) $[Pt(en)Cl_2]$; (c) $[Pt(en)Cl_2][Pt(en)Cl_4]$. (Reprinted with permission from *Inorg. Chem.*, 1992, **31**, 4281. Copyright (1992) American Chemical Society.)

Thioethers form a range of complexes (R_2Se and R_2Te behave similarly but have been less studied) [117]:

$$PdX_4^{2-} \xrightarrow{R_2Q} \textit{trans}\text{-}Pd(R_2S)_2X_2 \qquad (Q = S, Se, Te)$$

In $Pd(Et_2Se)_2Cl_2$, Pd–Se is 2.424 Å, Pd–Cl 2.266 Å

$$MI_2 \xrightarrow{C_4H_8S} \textit{trans}\text{-}MI_2(C_4H_8S)_2 \qquad (M = Pd, Pt)\ [118]$$

$$PtCl_4^{2-} \xrightarrow[(2\,mol)]{R_2S} \textit{trans}\text{-}Pt(R_2S)_2Cl_2 \xrightarrow[R_2S]{exc.} \textit{cis}\text{-}Pt(R_2S)_2Cl_2$$

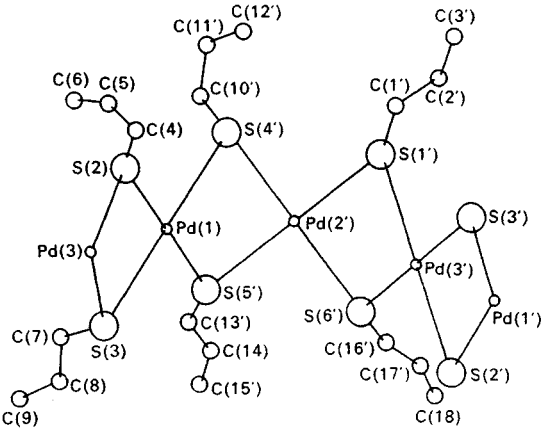

Figure 3.67 Part of the hexameric $[Pd(SPr^i)_2]_6$ molecule showing square-planar coordination of palladium. (Reproduced with permission from *Acta Crystallogr. Sect. B*, 1968, **24**, 1623.)

The structures of the *cis*- and *trans*-isomers of $Pt(1,4\text{-thioxane})_2Cl_2$ have been determined. The Pt–S distance (2.298 Å) is longer in the *trans*-isomer than in the *cis*-form (2.273 Å) showing the *trans*-influence of thioxane to be greater than that of chloride [119].

The two tetrahydrothiophen complexes above are isostructural [118]. Cationic complexes can be made

$$cis\text{-}Pt(Me_2S)_2Cl_2 \xrightarrow[1\text{ mol}]{AgNO_3/SMe_2} [Pt(Me_2S)_3Cl]NO_3$$

$$Pt(OH)_2 \xrightarrow[CF_3SO_3H]{Me_2S} [Pt(Me_2S)_4](CF_3SO_3)_2$$

The 4 : 1 complex has square planar coordination of platinum (Pt–S 2.317–2.321 Å); similar bond lengths are found in the corresponding complex with 1,4-thioxane [120]. Complexes with thiourea are important in Kurnakov's test (section 3.8.2); $Pdtu_4Cl_2$ has square planar coordination (Pd–S 2.33 Å).

Various bidentate ligands like dithiocarbamate afford monomeric square planar complexes; specific examples are $Pt(S_2CNEt_2)_2$ and $Pt(Se_2CNBu)_2$ (confirmed by X-ray). A similar structure is found for the dithiobenzoate $Pd(S_2CPh)_2$; one form of the dithioacetate is dimeric, a second form is a mixture of monomers and dimers.

Mixed mono-complexes can be made (Figure 3.68); the *trans*-influence of tertiary phosphine on the Pt–S bond is noticeable [121].

The series *cis*-$Pt(PhSC_2H_4SPh)X_2$ (X = Cl, Br, I) have been studied structurally (Table 3.12) and show little difference in the *trans*-influence of the halide ions on the Pt–S bond [122].

Crown thiaethers can form *mono*- or *bis*-complexes, depending upon the number of sulphurs in the ring (Figure 3.69).

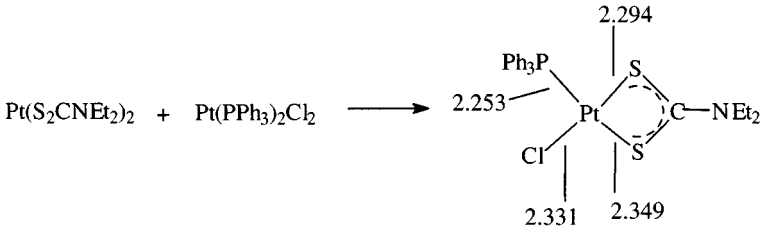

Figure 3.68 Synthesis and structure of $Pt(Ph_3P)Cl(S_2CNEt_2)$.

Table 3.12 Bond lengths (Å) in *cis*-$Pt(PhSC_2H_4SPh)X_2$

X	Pt–X	Pt–S
Cl	2.313–2.317	2.243–2.257
Br	2.430–2.434	2.248–2.249
I	2.601	2.262–2.268

To give some specific examples, in both $Pd(9S_3)_2^{2+}$ and $Pd(10S_3)_2^{2+}$ there is tetragonally distorted octahedral coordination; in the latter, Pd–S (equatorial) is 2.27 Å, Pd–S (axial) is 3.11 Å, the axial interaction being strong enough to give these complexes blue–green colours rather than the orange–yellow norm for square planar palladium(II). Brown $Pd(18S6)^{2+}$ has equatorial Pd–S distances of 2.31 Å and axial distances of 3.27 Å.

$Pt(9S_3)_2^{2+}$ is not isostructural with the palladium analogue but has square pyramidal coordination of platinum Pt–S (axial) 2.246–2.305 Å, (apical) 2.885 Å; $Pt(14S4)^{2+}$ has planar coordination (Pt–S 2.271–2.301 Å) with very distant axial contacts (3.680–3.721 Å) [123].

3.8.6 Complexes of ambidentate ligands

An ambidentate ligand has the choice of using two different types of donor atom. Two that have been extensively studied in their bonding to platinum and palladium are sulphoxides and thiocyanate.

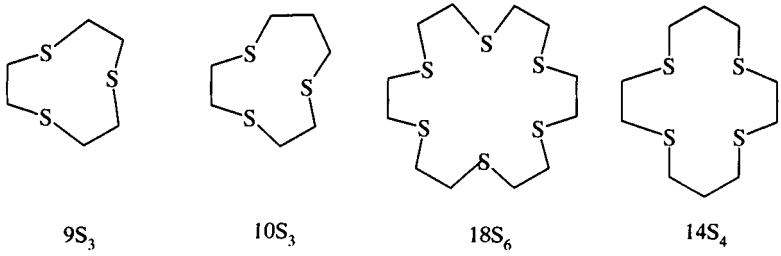

Figure 3.69 Crown thiaethers forming palladium and platinum complexes.

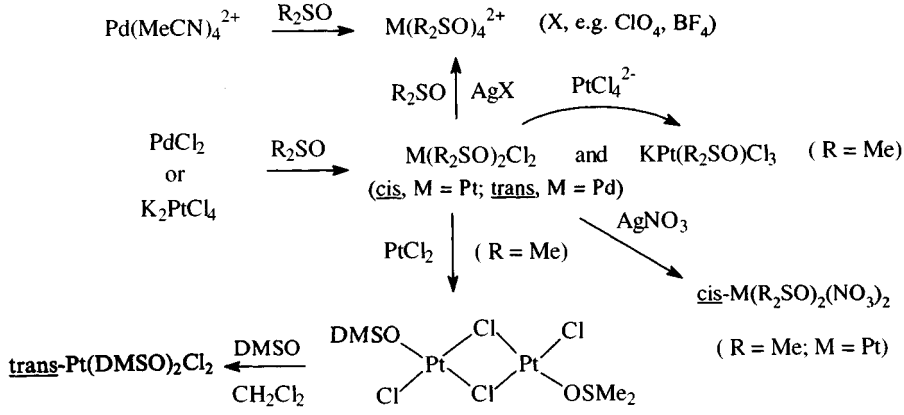

Figure 3.70 Synthesis of dialkylsulphoxide complexes.

Sulphoxide complexes [124]

Since the Pd^{2+} and Pt^{2+} ions are 'soft' acids, coordination by sulphur would be predicted. However, steric effects sometimes dictate bonding via oxygen. Some syntheses are shown in Figure 3.70.

The sterochemistry adopted between these complexes appears to be a balance between steric and electronic effects.

Thus $Pd(DMSO)_2Cl_2$ is the *trans*-isomer (S-bonded) while the platinum analogue is usually obtained as the S-bonded *cis*-isomer. The complex of Pr_2SO with $PtCl_2$ initially forms as the *trans*-isomer (presumably obtained as a result of the kinetic *trans*-effect for S-bonded sulphoxides) but isomerizes on standing to form an equilibrium mixture with the thermodynamically more stable *cis*-isomer. The isoamylsulphoxide complex $Pt[(Me_2CHCH_2CH_2)_2SO]_2Cl_2$ seems to be isolated as the (S-bonded) *trans*-isomer. The nitrate complexes $M(DMSO)_2(NO_3)_2$ have *cis*-(S-bonded) structures with monodentate nitrates (X-ray) (Figure 3.71) while the cationic complexes $[M(DMSO)_4]^{2+}X_2$ (X, e.g. BF_4, ClO_4) contain two S- and two O-bonded sulphoxides (*cis*-configuration presumably on steric grounds.

Steric crowding increases as bigger alkyl groups are introduced so that $[Pt[(Me_2CHCH_2CH_2)_2SO]_4](ClO_4)_2$ has only O-bonded sulphoxides (IR). IR spectra can be used to distinguish between S- and O-bonded sulphoxide:

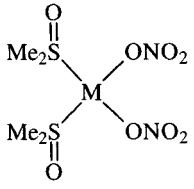

Figure 3.71 The coordination geometry of $M(DMSO)_2(NO_3)_2$ (M = Pd, Pt).

Figure 3.72 IR spectra of $[Pt(DMSO)_4](ClO_4)_2$ in the ν(S–O) region (the broad band at 1100 cm^{-1} is owing to the perchlorate group). (Reprinted with permission from *Inorg. Chem.*, 1972, **11**, 1280. Copyright (1972) American Chemical Society.)

when S-bonded, ν(S=O) increases from the free ligand value (*c.* 1050 cm^{-1}) to 1100–1160 cm^{-1}, whereas when the sulphoxide is O-bonded, ν(S–O) decreases into the region 900–960 cm^{-1} (Figure 3.72).

Crystallographic data can be used to draw up a *trans*-influence series. Comparing the Pt–Cl bond lengths in the compounds in Figure 3.73 shows that DMSO has a greater lengthening effect than the picoline, which in turn produces a slightly greater effect than chloride.

A synthetic route for the two picoline complexes relies on the fact that when the base was added to *cis*-$Pt(DMSO)_2Cl_2$, the *trans*-isomer is formed first. On standing, partial isomerization occurs to the *cis*-form, which can

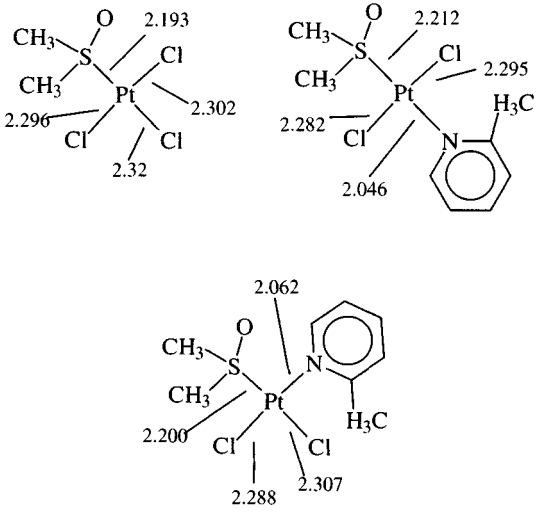

Figure 3.73 Structures of platinum complexes of DMSO.

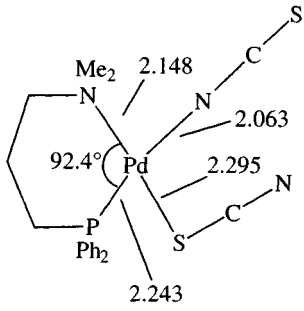

Figure 3.74 The structure of $Pd[Me_2N(CH_2)_3PPh_2](NCS)(SCN)$.

be induced to crystallize first by adding water.

$$cis\text{-}Pt(DMSO)_2Cl_2 \xrightarrow[DMSO]{L} trans\text{-}Pt(DMSO)LCl_2 + cis\text{-}Pt(DMSO)LCl_2$$

Thiocyanates [125]
Reaction of $PdCl_4^{2-}$ with KNCS leads successively to a precipitate of $Pd(SCN)_2$ and the soluble salt $K_2Pd(SCN)_4$ (square planar, Pd–S 2.31–2.39 Å). This reacts with Ph_3As to form the S,S-bonded $Pd(SCN)_2(AsPh_3)_2$ (kinetic product), which on heating gives the thermodynamically more stable N,N-bonded isomer:

$$K_2Pd(SCN)_4 \xrightarrow{AsPh_3} Pd(SCN)_2(AsPh_3)_2 \qquad (IR\ 2119\,cm^{-1})$$

$$\xrightarrow{solid} Pd(NCS)_2(AsPh_3)_2 \qquad (IR\ 2089\,cm^{-1})$$

Similar isomerizations have been noted for a number of complexes. As with metal nitrosyls, IR spectra can be used to indicate the manner of bonding, but there is an 'overlap' region around 2080–2100 cm^{-1} where ν(C–N) is found for both N- and S-bonded thiocyanates (additionally, S-bonded thiocyanates usually give a much sharper ν(C–N) band). ^{14}N NQR has been shown to be a reliable discriminator, but X-ray diffraction is ultimately the most reliable method.

In many cases, it has been found that π-bonding ligands favour S-bonding. In a complex with both N- and S-bonded thiocyanate (Figure 3.74) the N-bonded group is *trans* to P while the sulphur-bonded thiocyanate is *trans* to the 'harder' nitrogen ('anti-symbiosis').

However, the energy difference between N- and S-bonded thiocyanate is very small and is influenced by an interplay of several factors: steric effects, solvent and the counter-ion in ionic complexes. To illustrate the last point, in complexes $[Pd[Et_2N(CH_2)_2NH(CH_2)_2NH_2]NCS]^+$, the PF_6^- salt is N-bonded, as it is in the unsolvated BPh_6^- salt. However, though the acetone solvate of the tetraphenylborate is N-bonded, the methanol solvate is S-bonded [126].

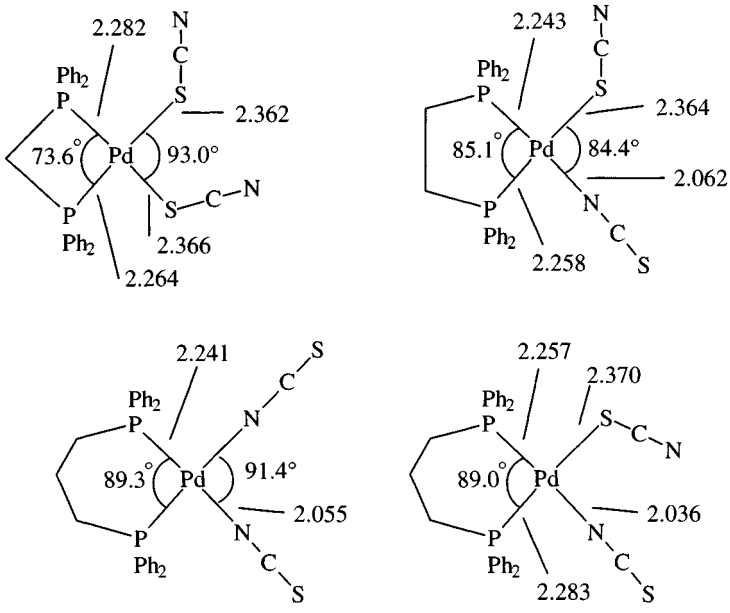

Figure 3.75 The structures of $Pd[Ph_2P(CH_2)_nPPh_2](NCS)_2$ ($n = 1$–3).

In a classic study (1975) it was shown that in the series $Pd[Ph_2P(CH_2)_n$-$PPh_2](NCS)_2$ ($n = 1$–3) the bonding of the thiocyanate changes from all-S to all-N coordinated as n increases (Figure 3.75) [127].

Subsequently it was shown that the P–Pd–P angles were essentially the same as in the corresponding chloride complexes (section 3.8.3): as a result, as the P–Pd–P angle increases, concomitant upon the increase in the length of the methylene chain, steric effects enforce N-bonded thiocyanate, which is less sterically demanding that the non-linear Pd–SCN linkage (favoured on HSAB considerations since Pd^{2+} is a 'soft' acid and sulphur is a 'soft' base).

Subsequent ^{31}P NMR study of solutions indicated that a mixture of isomers was present, with a distribution strongly dependent upon solvent; therefore, the energy difference between isomeric molecules was small. Moreover, the N,S-bonded isomer of the $Ph_2P(CH_2)_3PPh_2$ complex was also isolated in the solid state, as well as being found to be the predominant isomer in some solvents (DMF, Me_2CO, CH_2Cl_2). The isolation of the N,N-bonded isomer may have been a fortuitous success with this particular ligand, as it has not been achieved with other chelating ligands.

Two isomers have again [128] been obtained (S,S- and N,S-form) with the ligand dpbz (bis(diphenylphosphino)benzene) (Figure 3.76).

Such thiocyanate complexes are usually made by reaction of the ligand (L–L) with $Pd(SCN)_4^{2-}$ in a solvent like ethanol. A substantial amount of the Magnus-type salt $[Pd(L–L)_2][Pd(SCN)_4]$ is often produced, convertible to the neutral $Pd(L–L)(NCS)_2$ by dissolution in hot DMF and reprecipitating with water.

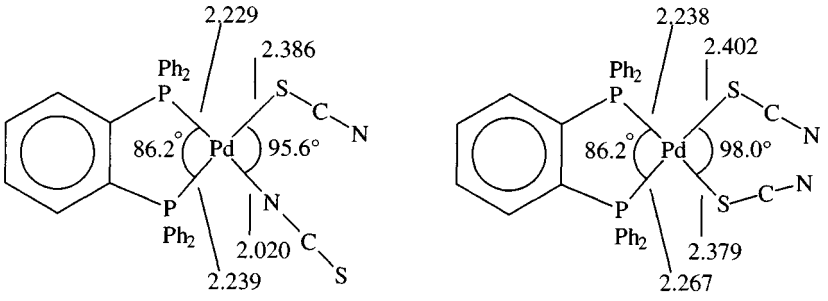

Figure 3.76 Isomers of $Pd[C_6H_4(PPh_2)_2](NCS)_2$.

It now appears that the most usual coordination mode in *cis*-di(thiocyanate) complexes is one N-bound and one S-bound thiocyanate, as an angular Pd–SCN bond minimizes interaction with the other bound thiocyanate and with the other ligands.

Most of the studies of ambidentate behaviour among thiocyanates concern palladium complexes; a recent report [129], however, investigated $Pt(bipy)(NCS)_2$

$$Pt(bipy)Cl_2 \xrightarrow[2.\,KSCN/H_2O]{1.\,AgClO_4/DMSO} Pt(bipy)(SCN)_2 \qquad \text{yellow, IR } 2119,\ 2131\ cm^{-1}$$

$$\xrightarrow{150°C} Pt(bipy)(NCS)_2 \qquad \text{red, IR } 2117\ cm^{-1}\ \text{(broad)}$$

The yellow form is stable at room temperature but isomerizes on warming in the solid state or solution. EXAFS measurements indicate that the yellow form has Pt bound to N and S (i.e. the thiocyanate is S-bonded) while the red form has no Pt–S bonds (Figure 3.77); therefore, the thiocyanate is N-bonded (there are also indications of distant Pt–Pt contacts (3.2 Å), possibly by 'stacking' of the planar $Pt(bipy)(NCS)_2$ units).

3.8.7 *Stability of* cis *and* trans-*isomers* [130]

For complexes like PtL_2X_2 (X = halogen; L = NH_3, PR_3, etc.) where *cis*- and *trans*-isomers exist, the *trans*-isomer is usually thermodynamically more stable. The *cis*-isomer may be formed first in a reaction and, in the case of platinum, may be relatively inert to substitution. (Thermodynamic data are relatively scarce; *trans*-$Pt(NH_3)_2Cl_2$ is some 13 kJ mol^{-1} more stable than the *cis*-isomer.)

Isomerization frequently occurs on heating. Solid *cis*-$Pt(NH_3)_2Br_2$ turns into the *trans*-isomer at 250°C while solid *cis*-$Pt(PMe_2Ph)_2MeCl$ also isomerizes on heating. These are presumably intramolecular processes involving pseudo tetrahedral intermediates. Some *trans*- to *cis*-isomerizations occur: solid *trans*-$Pt(Et_2SO)pyCl_2$ turns into the *cis*-isomer at 134°C, while

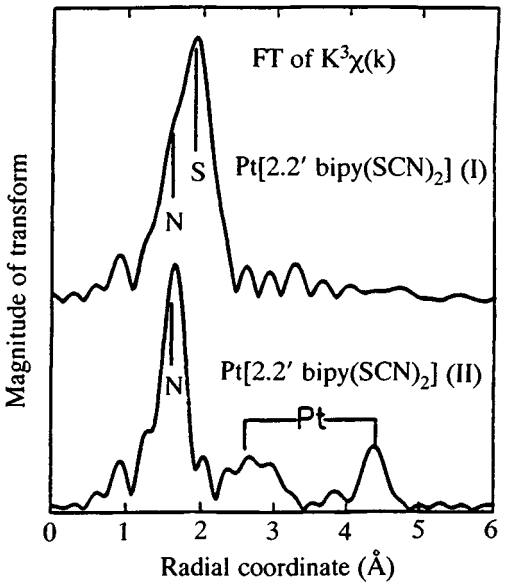

Figure 3.77 EXAFS spectra of the isomers of Pt(bipy)(NCS)$_2$. (Reprinted with permission from *Inorg. Chem.*, 1992, **31**, 1752. Copyright (1992) American Chemical Society.)

rans-Pt(PPr$_3$)$_2$Cl$_2$ partly turns into the *cis*-isomer in benzene solution. (In contrast the palladium analogue does not isomerize.) The π-bonding effects have been used to explain the unexpectedly high stability of some *cis*-isomers, as more d orbitals are involved in dπ–pπ overlap (Figure 3.78).

Thermal isomerizations can be used in the synthesis of, in particular, Pt(PR$_3$)$_2$X$_2$ isomers [131a] (section 3.8.3). *Trans*-Pt(PR$_3$)$_2$X$_2$ (X = Cl,

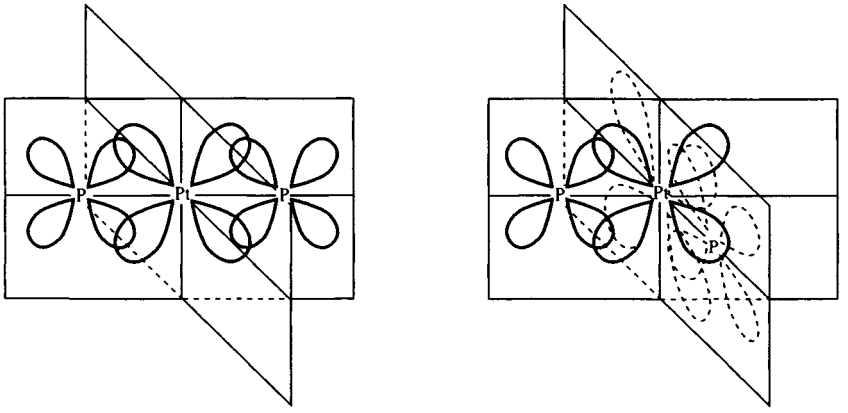

Figure 3.78 Postulated π-bonding in *cis*- and *trans*-phosphine complexes. (Reproduced with permission from S.A. Cotton and F.A. Hart, *The Heavy Transition Elements*, Macmillan Press Ltd, 1975, p. 119.)

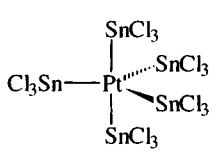

Figure 3.79 The trigonal bipyramidal $[Pt(SnCl_3)_5]^{3-}$.

R = Bu; X = Br, R = Et, Pr, Bu; X = I; R = Et, Pr) can be prepared by solid state isomerization of the *cis*-form at a temperature just below the melting point; by comparison, complexes of trimethyl- and triphenylphosphine decompose without change. Isomerization of $PtCl_2(EtCN)_2$ has likewise been studied [131b].

3.8.8 Five-coordinate compounds

Despite the fact that PtL_3X_2 and PtX_5^{3-} species have an 18-electron configuration, 5-coordinate palladium(II) and platinum(II) compounds are rare. One of the first examples to be established was $Pt(SnCl_3)_5^{3-}$

$$PtCl_4^{2-} \xrightarrow[2.\ Ph_3PMe+MCl]{1.\ SnCl_2/HCl} (Ph_3PMe)_3[Pt(SnCl_3)_5]$$

It has a tbp structure (Figure 3.79) with Pt–Sn 2.553 Å (axial) and 2.5722 Å (equatorial) (in the corresponding $(Me_4N)_3Pt(GeCl_3)_5$, the Pt–Ge distances are 2.400 and 2.434 Å, respectively); the shorter axial bond lengths are ascribed to differences in Pt–Sn π-bonding.

^{195}Pt and ^{119}Sn NMR data show $Pt(SnCl_3)_5^{3-}$ to be non-rigid (on the NMR timescale) down to 183 K, owing to an intramolecular process, possibly a 'Berry twist' mechanism [132].

Stable anionic complexes $[Pt(SnCl_3)_3L_2]^-$ are formed by tertiary phosphines and arsines with small cone angles (L = PR_3, AsR_3; R = Me, Et, OEt), confirmed by X-ray diffraction for $[Pt(SnCl_3)_3(AsMe_3)_2]^-$, which has axial arsines (Pt–As 2.427–2.445 Å; Pt–Sn 2.579–2.614 Å). With larger ligands, steric constraints mean that planar species like *trans*-$Pt(SnCl_3)_2[P(OPh)_3]_2$ are obtained [133]. In solution, $[Pt(SnBr_3)_5]^{3-}$ is unstable with respect to dissociation into $[PtBr_2(SnBr_3)_2]^{2-}$ and $[PtBr_3(SnBr_3)]^{2-}$ in the absence of added $SnBr_2$ [134]; salts $M_3[Pt(SnBr_3)_5]$ (M = Bu_4N, $PhCH_2PPh_3$) have been prepared in the solid state.

Some 5-coordinate phosphite complexes (fluxional at room temperature) exist

$$PtCl_2 \xrightarrow[2.\ NaBPh_4]{1.\ (MeO)_3P/MeOH} Pt[P(OMe)_3]_5^{2+}(BPh_4)_2$$

Again, steric effects prevent more than four bulky phosphites coordinating [135].

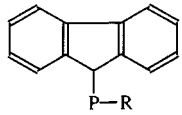

I, R = Et; II, R = Me

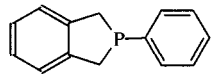

III

Figure 3.80 Phosphine ligands forming the 5-coordinate palladium and platinum complexes.

A number of tertiary phosphine complexes with bulky ligands (Figure 3.80) have modified square pyramidal structures, examples being $M(I)_3Br_2$, $Pt(II)_3Br_2$ and $Pd(III)_3Br_2$ (all X-ray) [136].

One crystalline form of *trans*-$Pd(PMe_2Ph)_2I_2$ has a pseudo-sp structure in the solid state as an iodine atom from a neighbouring molecule occupies a distant 'axial' position [137a]. Other complexes of PMe_2Ph, $M(PMe_2Ph)_3X_2$ (M = Pd, Pt; X = halogen), are likely to be 5-coordinate, confirmed for $Pd(PMe_2Ph)_3Cl_2$ [89]. $[Pd(tmpp)_2]^{2+}$ exhibits short axial Pd–O bonds (2.632–2.671 Å) and is regarded as a distorted octahedral complex [137b].

Complexes of bulky substituted phenanthrolines $[Pt(N{-}N)LX_2]$ (L, X both monodentate; N–N, e.g. 2,9-dimethyl-1,10-phenanthroline) can be 5-coordinate tbp when a good π-acceptor (e.g. C_2H_4) is present or 4-coordinate with monodentate phenanthrolines. Hartree–Fock calculations indicate that the π-acceptors reduce the electron density at platinum so that the metal can accept charge from another donor. Species of this kind may be involved in alkene hydrogenation [138].

3.8.9 The trans-*effect*

In the 1920s, the Russian chemist Il'ya Il'ich Chernyaev systematized reactions of complexes of several metals, particularly platinum(II and IV), by noting that a ligand bound to a metal ion influenced the ease of replacement of the group *trans* to it in the complex [139].

The *trans*-effect has been defined [140] as 'the effect of a coordinated group upon the rate of substitution reactions of ligands opposite to it. Metals in which the rate influence of opposite, or *trans*-groups, is definitely greater than the influence of adjacent, or *cis* groups, will be considered to show a *trans*-effect'. The *trans*-effect is, therefore, a kinetic phenomenon, related presumably to the transition state, as well as the ground state, in the substitution reaction. It is not the same as *trans*-influence. The *trans*-influence of a ligand is a measure of the effect of a ligand on the strength of a bond opposite to it in a complex: it is a ground-state effect, which can be measured in terms of lengthening of bonds (X-ray diffraction) or vibrational spectra (sections 3.8.10 and 3.8.11).

The trans*-effect and substitution reactions*

Square planar complexes of palladium(II) and platinum(II) readily undergo ligand substitution reactions. Those of palladium have been studied less but appear to behave similarly to platinum complexes, though around five orders of magnitude faster (ascribable to the relative weakness of the bonds to palladium).

For a substitution reaction of the type

$$PtL_3X + Y \rightarrow PtL_3Y + X$$

the rate law is generally found to be of the form

$$\text{Rate} = \frac{-d[PtL_3X]}{dt} = (k_1 + k_2[Y])[PtL_3X] = k_1[PtL_3X] + k_2[Y][PtL_3X]$$

suggesting two competing pathways.

The k_1 term is independent of Y and would, therefore, appear to be dissociative, but it is in fact found to be solvent-dependent and so it is thought to be associative. (It is also found to be sensitive to steric effects in the same manner as the k_2 pathway.) A plausible pathway for the k_1 route is slow solvolysis followed by fast substitution

$$PtL_3X + S \xrightarrow{\text{slow}} PtL_3S + X \xrightarrow[Y]{\text{fast}} PtL_3Y + S$$

The k_2 term suggests a simple bimolecular process in which nucleophilic attack by Y leads to a S_N2 reaction. Associative paths will involve a 5-coordinate (sp or tbp) intermediate, and the relative rarity of isolable 5-coordinate platinum(II) species – compared with 4-coordinate – is not inconsistent with their involvement as reactive intermediates (Figure 3.81).

Retention of configuration occurs in these substitution reactions, as expected for a process involving a 5-coordinate intermediate in which the entering and leaving ligands are simultaneously bound.

Kinetic study [141] of complexes of the type *trans*-$Pt(PEt_3)_2XCl$ was of great value in establishing the strong *trans*-effect of hydride (Table 3.13); examination of the data for a wide range of reactions gives rise to a series

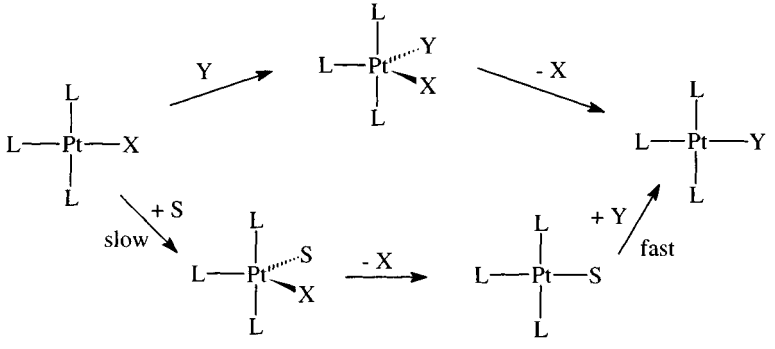

Figure 3.81 Pathways for substitution of a square planar species PtL_3X.

Table 3.13 Comparison of the effect of the *trans*-ligand on substitution of Cl by py in *trans*-$PtClX(PEt_3)_2$ at 25°C

X	k_1 (s^{-1})	k_2 ($M^{-1}s^{-1}$)
PEt_3	1.7×10^{-2}	3.8
H^- [a]	1.8×10^{-2}	4.2
Me^-	1.7×10^{-4}	6.7×10^{-2}
Ph^-	3.3×10^{-5}	7.5×10^{-4}
Mesityl	1.7×10^{-6}	3.7×10^{-4}
Cl^-	1.0×10^{-6}	4.0×10^{-4}

[a] For H^-, measured at 0° (reaction too fast to measure at 25°C).

with *trans*-effect defined as the ability of a coordinated ligand to labilize a ligand *trans* to it.

The *trans*-effect is, therefore, a kinetic labilizing effect rather than a thermodynamic one. An approximate series is:

$$CN^-, CO, C_2H_4 > PR_3, H^- > Me^- > tu \sim R_2S > NO_2^-, I^- > SCN^- > Br^- > Cl^- > \text{pyridine} > NH_3 > OH^- > H_2O$$

Two examples of steric effects deserve attention. In aryl complexes *cis*-$Pt(PR_3)_2ArCl$, introducing *ortho*-substituents into the phenyl group slows down substitution considerably, as these block the position of attack (Figure 3.82).

From the data in Table 3.14, note the greater range of values of k for the *cis*-isomers, showing their greater sensitivity to steric effects (the similarity of the value for the phenyl and *p*-tolyl derivatives may also be noted).

In contrast, the *trans*-isomers are much less affected by the substituents in the benzene ring, as there is interaction in the transition state [142].

Comparison of results for complexes of tridentate amines $R_2N(CH_2)_2NH(CH_2)_2NR_2$ show similar effects. With dien (R = H), rapid substitution of chloride in $Pt(dien)Cl^+$ by bases occurs at room temperature; however with Et_4dien (R = Et) the reaction is considerably slowed, since the four ethyl groups crowd the metal above and below the plane of the molecule (Figure 3.82) making nucleophilic attack harder. Such a complex can be attacked more easily by a small nucleophile rather than a 'better' nucleophile which happens to be larger [89].

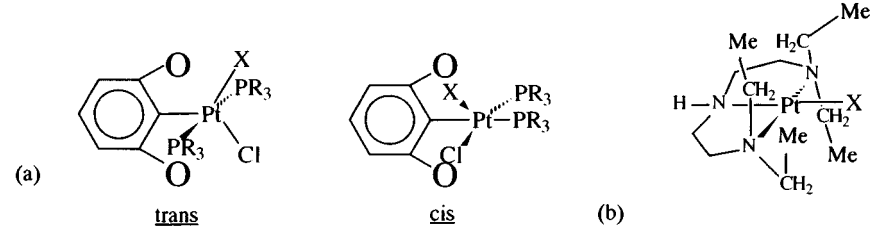

Figure 3.82 (a) The effect of *ortho*-substituents on substitution reactions of *cis*-$Pt(PR_3)_2ArCl$ complexes; (b) the effect of alkyl substituents on substitution reactions of dien complexes.

Table 3.14 Rates of attainment of equilibrium in the reaction between $Pt(PR_3)_2RCl$ and pyridine

R	k_1 (s^{-1}) *cis*-isomer (0°C)	k_1 (s^{-1}) *trans*-isomer (25°C)
Me	6.0×10^{-2}	1.7×10^{-4}
Ph	3.8×10^{-2}	3.3×10^{-5}
o-Tolyl	8.6×10^{-5}	6.7×10^{-6}
p-Tolyl	5.0×10^{-2}	–
Mesityl	4.2×10^{-7}	1.2×10^{-6}

Theoretical explanation of the *trans*-effect (and *trans*-influence) has centred on two theories, one based on σ-bonding the other on π-bonding. The σ-bonding argument considers two *trans*-ligands sharing a metal p orbital (Figure 3.83).

A strong σ-donor contributes high electron density, weakening the bond *trans* to it. This is essentially a ground-state argument, as in a 5-coordinate reaction intermediate the two groups will not be competing for electron density in just this one orbital. This would give rise to a σ-bonding order such as $H^- > PR_3 > SCN^- > I^-$, NCS, CO, $CN^- > Br^- > Cl^- > NH_3 > OH^-$.

One or two ligands such as CO and CN that have high observed *trans*-effects (and therefore are out of place in the above series) do possess empty orbitals that can act as π-acceptors to remove electron density from the metal ion, making the region *trans* to the ligand electron deficient and able to be attacked by the nucleophile in the transition state (Figure 3.84).

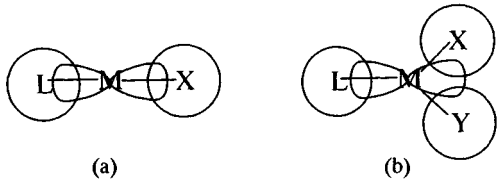

Figure 3.83 (a) Ground state weakening; (b) Weakening reduced with lessening competition in the transition state.

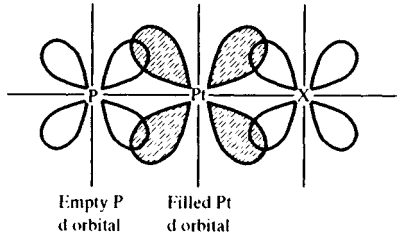

Figure 3.84 Effect of a π-bonding ligand in acting as a π-acceptor. (Reproduced with permission from S.A. Cotton and F.A. Hart, *The Heavy Transition Elements*, published by Macmillan Press Ltd, 1975, p. 118.)

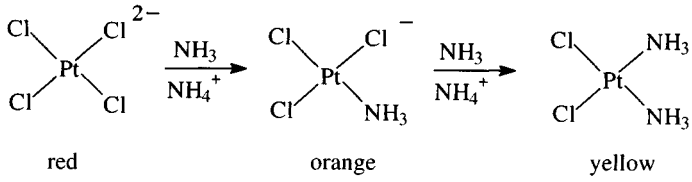

Figure 3.85 Synthesis of *cis*-$Pt(NH_3)_2Cl_2$.

This would give rise to an order of the kind $R_2C{=}CR_2$, $CO > CN^- > NO_2^- > SCN^- > I^- > Br^- > NH_3 > OH^-$. Therefore, a combination of σ- and π-effects can be considered to give rise to the observed *trans*-effect series.

Explanations of the *trans*-effect and *trans*-influence have considered σ- and π-bonding, often to the point of mutual exclusion.

Theories based on σ-effects consider that the more electronegative a ligand the more polarization of the metal occurs, weakening the bond *trans* to it. This can alternatively be viewed in terms of electronic transmission via a σ-type (p) orbital shared by the two ligands.

A π-bonding explanation notes that several ligands high in the *trans*-effect series are good π-acceptors and thus siphon off π-density, making the region *trans* to it electron deficient and thus attractive to ligands that are electron rich.

Synthetic applications of the trans-*effect* [139b, 143]

The classic application of the *trans*-effect lies in the synthesis of the *cis*- and *trans*-isomers of $Pt(NH_3)_2Cl_2$, known as Peyrone's salt and Reiset's salt after their respective discoverers in 1844.

The *cis*-isomer is made by reacting $PtCl_4^{2-}$ with ammonia solution (Figure 3.85).

Because Cl^- has a stronger *trans*-effect than NH_3, a group opposite to Cl^- is replaced in the second substitution. Similarly, in the synthesis of the *trans*-isomer by heating $Pt(NH_3)_4^{2+}$ with Cl^-(Figure 3.86), it is the ligand *trans* to chloride that is again replaced in the second step.

The *cis*- and *trans*-isomers of $[Pt(NH_3)(NO_2)Cl_2]^-$ have been synthesized from $PtCl_4^{2-}$ merely by choice of the order of ligand substitution (Figure 3.87). (In the second step, chloride *trans* to chloride is more labile.) The second substitution is dictated by NO_2 having a higher position in the *trans*-effect series than chloride [144].

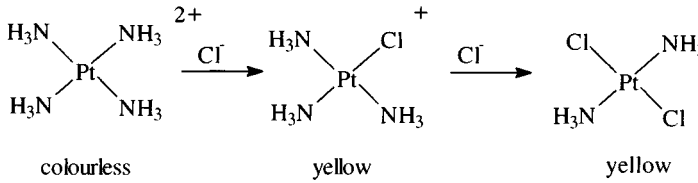

Figure 3.86 Synthesis of *trans*-$Pt(NH_3)_2Cl_2$.

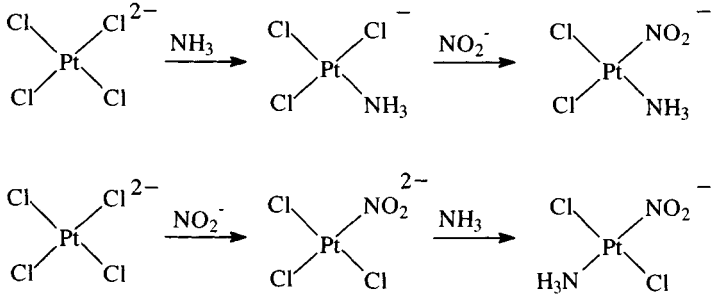

Figure 3.87 Synthesis of the isomers of $[Pt(NH_3)(NO_2)Cl_2]^-$.

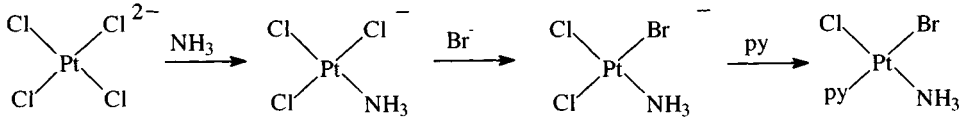

Figure 3.88 Synthesis of the first isomer of $PtClBr(NH_3)py$.

Square planar complexes of the type MABCD have three geometric isomers and in several cases all have been synthesized. Therefore, the isomers of $[PtClBr(NH_3)py]$ can be synthesized as shown in Figures 3.88–3.90.

The second substitution relies on the (observed) fact that anionic ligands (e.g. Cl^-) are more readily replaced than neutral ones (e.g. NH_3), so that chloride *trans* to chloride is substituted rather than NH_3 *trans* to chloride. In the third step, the chloride *trans* to bromide is replaced, in keeping with the *trans*-effect order Br > Cl. In Figure 3.89, the second step again relies on the observed kinetic weakness of the Pt–Cl bond, while the third substitution again involves replacement of the chloride *trans* to the group highest in the *trans*-effect series. The third isomer is produced by a sequence in which the second step is again an example of the kinetic weakness of the Pt–Cl

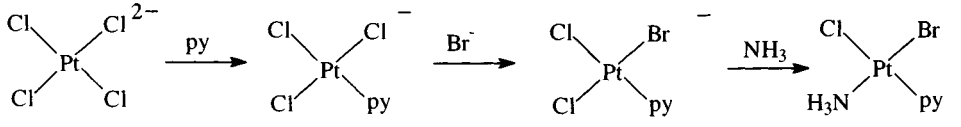

Figure 3.89 Synthesis of the second isomer of $PtClBr(NH_3)py$.

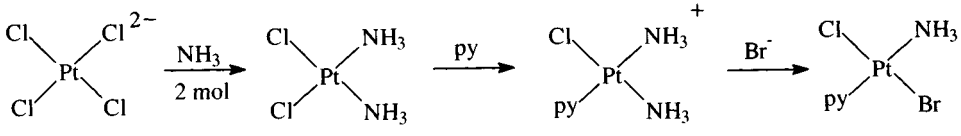

Figure 3.90 Synthesis of the third isomer of $PtClBr(NH_3)py$.

Table 3.15 Pt–Cl bond lengths in ions $PtLCl_3^-$

L	Pt–Cl *trans* to L	Pt–Cl *cis* to L	Pt–L
PEt_3	2.382	2.299–2.302	2.215 (P)
C_2H_4	2.340	2.303	2.022[a]
NH_3	2.321	2.30–2.32	2.06 (N)
2,6-Me_2py	2.309	2.302	2.024 (N)
CO	2.289	2.290–2.294	1.82 (C)
MeCN	2.266	2.293–2.301	1.960 (N)
Me_2SO	2.309	2.271–2.275	2.185 (S)
py	2.305	2.293–2.299	2.018 (N)

[a] To midpoint of C–C bond.

bond compared with the Pt–NH_3 bond. The *trans*-effect series again predicts the replacement of the group *trans* to Cl in the third step [145].

Similarly, all three isomers have been isolated for $PtBr(NO_2)NH_3(py)$ and $PtCl(NO_2)(NH_3)(MeNH_2)$ while Chernyaev used the synthesis of all three isomers of $[Pt(NH_3)py(NH_2OH)(NO_2)]^+Cl^-$ as evidence for a square planar geometry [146].

3.8.10 Structural evidence for trans*-influence*

A considerable amount of X-ray data has now been accumulated to support the concept of *trans*-influence. In a series of ions, $PtLCl_3^-$ (L = neutral ligand), the Pt–Cl bond *trans* to the neutral ligand displays much more sensitivity to L than do the *cis*-chlorines (Table 3.15) [147].

Variation of *cis*-bond lengths has been noted in some cases and is believed to reflect steric interaction. Therefore, in the series $PtX(PEt_3)_3^+$ (X = H, Cl, F) the *trans*-bond to X shows a dependence upon the electronegativity of X, while the *cis*-Pt–P bond shows no such dependence (Figure 3.91) [148], instead increasing as X becomes larger.

Similar dependence is noted in the complexes $PtH_xCl_{2-x}(PPr^i_3)_2$ ($x = 0, 1, 2$) where the Pt–P bond increases by 0.04 Å for each successive replacement of hydrogen by the bulkier chlorine (Figure 3.92) [149].

A number of mainly *trans*-$M(PR_3)_2XY$ compounds (X, Y = Cl, Me, H, Br, Ph, I) have been studied (Figure 3.93) [150].

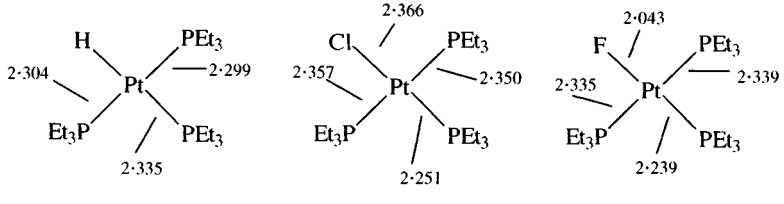

Figure 3.91 Bond lengths in the ions $[PtX(PEt_3)_3]^+$ (X = H, Cl, F).

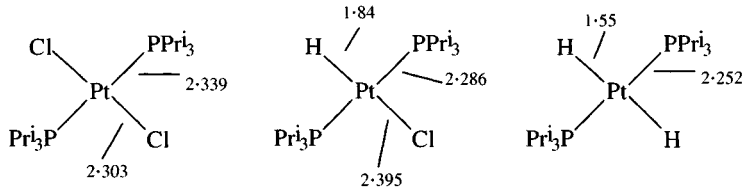

Figure 3.92 Bond lengths in the compounds $PtH_xCl_{2-x}(PPr^i_3)_2$.

They display the considerable *trans*-influence of hydride and aryl groups (the Pt–Cl bond lengths should be compared with the value of *c.* 2.31 Å in $PtCl_4^{2-}$). The Pt–P bond lengths are more insensitive to the phosphine, but by synthesis of *cis*-$Pt(PR_3)(PR'_3)Cl_2$ [150] complexes, it has been possible to study the effect of electron-withdrawing substituents on the Pt–P bond, as well as on the *trans*-influence of the phosphine (Figure 3.94).

Very bulky ligands, of course, cause steric effects. The similarity of the Pt–P bond lengths in *trans*-$Pt(PR_3)_2H_2$ (R = Me, cy) suggest that the bonding is similar in these two compounds (Table 3.16 and Figure 3.95)

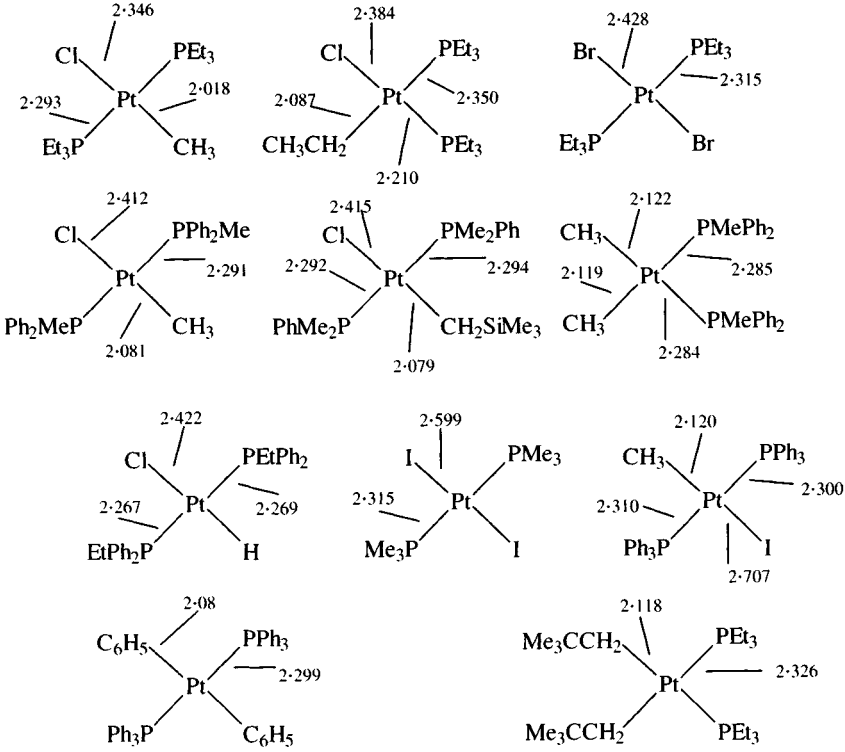

Figure 3.93 Bond lengths in compounds *trans*-$Pt(PR_3)_2XY$.

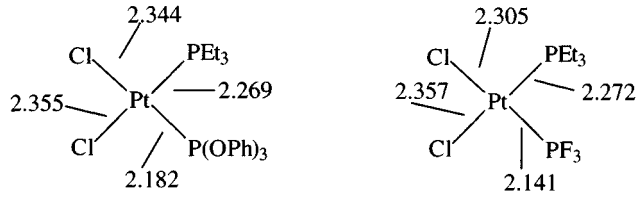

Figure 3.94 Bond lengths in compounds *cis*-$Pt(PR_3)(PR'_3)Cl_2$.

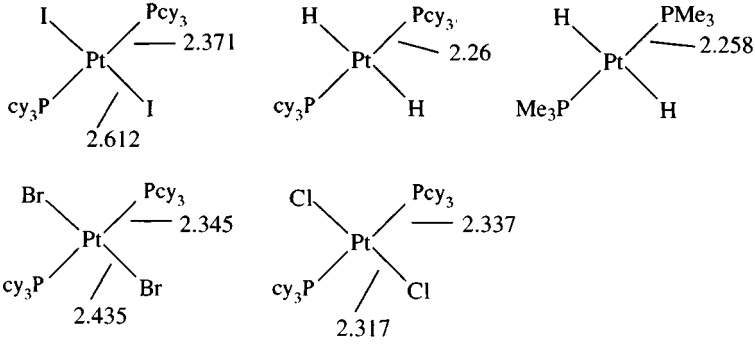

Figure 3.95 Bond lengths in compounds *trans*-$Pt(Pcy_3)_2X_2$ (X = H, halogen).

but on passing to the iodide *trans*-$Pt(Pcy_3)_2I_2$, the long Pt–P (and Pt–I) bond lengths indicate crowding; chemical evidence of this is that, on heating, the iodide eliminates a molecule of phosphine affording the halogen-bridged dimer $[Pt(Pcy_3)I_2]_2$.

Careful comparison of Pt–P bond lengths for the series *trans*-$Pt(Pcy_3)_2X_2$ (X = H, Cl, Br, I) with those for *trans*-$Pt(PR_3)_2X_2$ (PR_3 = PMe_3 or PEt_3) shows a more definite increase in Pt–P with anion size for the cyclohexylphosphine complexes (Table 3.16) believed to be owing to intermolecular X···H and X···C non-bonded interactions arising from overcrowding [151].

A series of phosphine complexes with '*cis*-PtP_2Cl_2' geometries have been compared (Table 3.17).

The Pt–P (and Pt–Cl) bond lengths correlate with the electron-donating ability of the phosphine (Tolman's χ_i factor) rather than steric factors (the cone angle of the tertiary phosphine) [150b].

Table 3.16 Pt–P bond lengths for *trans*-$Pt(PR_3)_2X_2$ complexes (Å)

X	$Pt(Pcy_3)_2X_2$	$Pt(PR_3)_2X_2$
H	2.26	2.259 (R = Me)
Cl	2.337	2.30 (R = Et)
Br	2.345	2.315 (R = Et)
I	2.371	2.315 (R = Me)

Table 3.17 Phosphine *cis*-PtP_2Cl_2 complexes

	Pt–P (Å)	Pt–Cl (Å)	Cone angle (°)	$\sum X_i$
cis-$Pt(PEt_3)_2Cl_2$	2.258	2.361	130	5.4
cis-$Pt(PMe_3)_2Cl_2$	2.248	2.376	118	7.8
cis-$Pt(PMe(C_6F_5)_2)_2Cl_2$	2.236	2.344	130	16.4
cis-$Pt(PEt_3)(P(OPh)_3)Cl_2$	2.182	2.344	128	29.1
cis-$Pt(PEt_3)(PF_3)Cl_2$	2.141	2.305	104	54.6

Table 3.18 IR and NMR data for *trans*-$Pt(PEt_3)_2HX$

X	Cl	Br	I	NCS	$SnCl_3$	CN
ν (Pt–H) (cm^{-1})	2183	2178	2156	2112	2105	2041
δ (ppm) (hydride)	−16.9	−15.6	−12.7	−13.2	−9.2	−7.8

3.8.11 Spectroscopic evidence for trans-*influence*

Infrared

Study of a series of complexes *trans*-$Pt(PEt_3)_2HX$ shows a pronounced dependence of ν(Pt–H) upon the *trans*-ligand (Table 3.18).

Similarly, in complexes PtL_2Cl_2, the Pt–Cl stretching frequency is relatively insensitive to L in the *trans*-isomer but shows considerable dependence in the *cis*-isomer (Table 3.19) [100].

NMR evidence

Table 3.18 shows how the position of the low-frequency hydride resonance is affected by the *trans*-ligand, while study of a series of complexes *trans*-$[Pt(PMe_2Ph)_2(Me)L]^+$ and neutral *trans*-$Pt(PMe_2Ph)_2(Me)X$ shows the *trans*-influence of the ligand on $^2J(^{195}Pt-^1H)$ with better donors tending to reduce the value of J (Table 3.20) [152].

Platinum ammine complexes have been a fertile area for studying *trans*-influence. Table 3.21 lists data for a range of ammines showing how $^1J(^{195}Pt-^{15}N)$ depends upon the *trans*-atom [153]. (A further selection of data can be found in: R.V. Parish, *NMR, NQR, EPR and Mössbauer Spectroscopy in Inorganic Chemistry*, Ellis-Horwood, Chichester, 1991, pp. 76, 87.) Possibly the most detailed study (of complexes of tribenzylphosphine) examined over a hundred neutral and cationic complexes [154] (Table 3.22).

Table 3.19 ν (Pt–Cl) in complexes PtL_2Cl_2 (cm^{-1})

L	NH_3	PEt_3	Et_2S	py	$AsEt_3$
trans-Isomer	331.5	340	342	342.6	339
cis-Isomer	326	303, 281	330, 318	343, 328	314, 287.5
Average	326	292	324	335.5	301

Table 3.20 The *trans*-influence of ligands on $^2J(^{195}Pt-^1H)$ in *trans*-A^+ and *trans*-AX^a

L	X	J (Hz)
$SbPh_3$		55
PMe_2Ph		57
$P(OPh)_3$		58
PPh_3		60
CO		63
Py		74
PhCN		79
	Cl	85
	Br	83
	I	80

[a] A is $Pt(PMe_2Ph)_2$ MeL

Putting the ligands in order of their effect on the value of δ, the position of the hydride resonance, gives H $\gg$ CO, PR_3 > CN > tu > NO_2 > SMe_2 > SCN, I > Br > Cl > NH_3, py. A not dissimilar order is found for their effect on ν(Pt–H) in the IR spectrum (H $\gg$ CN > PR_3 > I > SCN ~ NO_2 ~ tu ~ CO ~ Cl > SMe_2 > Br > NH_3 > py). Data correlate well with those for other tertiary phosphines, e.g. Pcy_3.

A seminal paper [155] examined platinum–phosphorus NMR coupling constants in a series of *cis*- and *trans*-platinum(II and IV) complexes. The *trans*-influence had hitherto been explained in terms of $d\pi$–$p\pi$ bonding, in other words, such a mechanism dominated with *trans*-effect

Table 3.21 $J(^{195}Pt-^{15}N)$ values (Hz) for platinum(II) amine complexes

	NH_3 *trans* to			
	O	N	Cl	S
cis-$Pt(NH_3)_2Cl_2$			326	
trans-$Pt(NH_3)_2Cl_2$		278		
cis-$Pt(NH_3)_2(H_2O)_2^{2+}$	391			
trans-$Pt(NH_3)_2(H_2O)_2^{2+}$		312		
$Pt(NH_3)_4^{2+}$		287		
$Pt(NH_3)_3Cl^+$		281	331	
$Pt(NH_3)_3(H_2O)^{2+}$	376	299		
cis-$Pt(NH_3)_2tu_2^{2+}$				237
cis-$Pt(NH_3)_2tu_2^{2+}$				263
cis-$Pt(NH_3)_2(SCN)_2$				250
$Pt(NH_3)_3tu^{2+}$		277		243
$Pt(NH_3)_3SCN^+$		282		264
$Pt(NH_3)_3(Me_2SO)^{2+}$		303		243

Table 3.22 NMR and IR data [154] for complexes *trans*-$Pt(Pbz_3)_2HX$ and *trans*-$[Pt(Pbz_3)_2HL]^+$

X/L	ν(Pt–H) (cm^{-1})	δ (ppm)	J(Pt–H) (Hz)	J(Pt–P) (Hz)
H	1734	−2.4	800	–
Cl	2210	−17.36	1290	2969
Br	2221	−16.47	1345	2925
I	2192	−13.62	1359	2882
SCN	2203	−13.58	1186	
CN	2059	−8.69	776	
NH_3	2256	−18.16	1042	2928
Py	2290	−18.89	1022	2919
PPh_3	2140, 2123	−6.87	783	2717
Pbz_3	2145	−7.28	714	2682
$P(OPh)_3$	2165	−5.85	758	2620
SMe_2	2219	−13.30	1094	2820
CO	2207	−6.12	840	
tu	2205	−10.09	1134	
NO_2	2200	−12.09	1008	

and *trans*-influence. The results in Table 3.23 show that the ratio $J_{cis} : J_{trans}$ is similar in the platinum(II) and platinum(IV) complexes.

Since π bonding is believed to be more important in low oxidation states, as d orbitals contract with increasing oxidation state leading to poorer $d\pi$–$p\pi$ overlap, this would not be expected on the basis of a π-bonding mechanism. Similarly, one can compare J(Pt–P) for pairs of isomers in the +2 and +4 states; in a planar platinum(II) complex, the platinum 6s orbital is shared by four ligands whereas in an octahedral platinum(IV) complex it is shared by six ligands. Therefore, the 6s character is expected to be only 2/3 as much in the platinum(IV) complexes, correlating well with the J(Pt–P) values, which can be taken to be a measure of the σ-character in the bond.

Table 3.23 NMR coupling constants for platinum phosphine complexes [155]

	$J(^{195}Pt–^{31}P)$ (Hz)
cis-$PtCl_2(PBu_3)_2$	3508
cis-$PtBr_2(PBu_3)_2$	3479
cis-$PtI_2(PBu_3)_2$	3372
trans-$PtCl_2(PBu_3)_2$	2380
trans-$PtBr_2(PBu_3)_2$	2334
trans-$PtI_2(PBu_3)_2$	2200
cis-$PtCl_4(PBu_3)_2$	2070
trans-$PtCl_4(PBu_3)_2$	1462
cis-$PtCl_2[P(OEt)_3]_2$	5698
cis-$PtBr_2[P(OEt)_3]_2$	5662
cis-$PtI_2[P(OEt)_3]_2$	5472

Table 3.24 NMR coupling constants for platinum amine complexes [156]

	$J(^{195}Pt-^{15}N)$ (Hz)
cis-PtL_2Cl_2	351
cis-PtL_2Cl_4	249
trans-PtL_2Cl_2	290
cis-PtL_2Br_2	334
cis-PtL_2Br_4	223
trans-PtL_2Br_2	279

$L = C_{12}H_{25}NH_2$

Support for this view is found in the $^{195}Pt-^{15}N$ coupling constants for dodecylamine complexes of platinum(II) and platinum(IV), where π-bonding cannot of course occur, which exhibit similar trends (Table 3.24) [156].

As already mentioned, a purely π-bonding mechanism cannot account for the position of hydride in *trans*-effect and *trans*-influence series. Overall, therefore, a major role (though not necessarily the only one) for σ-bonding is implied.

3.9 Palladium(III) and platinum(III) compounds

Mononuclear complexes of palladium and platinum in the +3 oxidation state have only recently been unequivocally characterized [157]. The major advance has come in complexes with macrocyclic ligands such as 1,4,7-trithiacyclononane (ttcn) and 1,4,7-triazacyclononane (tacn) (Figure 3.96).

Complexes of the divalent metals $[M(ttcn)_2]^{2+}$ undergo electrochemical oxidation to paramagnetic $[M(ttcn)_2]^{3+}$. Red $[Pd(ttcn)_2]^{3+}$ has a tetragonally distorted octahedral structure (d^7, Jahn–Teller distortion) with Pd–S 2.356–2.369 Å (equatorial) and 2.545 Å (axial) in keeping with the ESR spectrum ($g_\perp = 2.049$, $g_{||} = 2.009$) which also displays ^{105}Pd hfs. Similarly, electrochemical oxidation of the palladium(II) tacn complex (at a rather lower

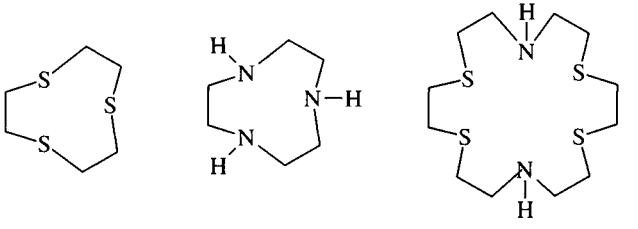

ttcn ($9S_3$) tacn $18[ane]N_2S_4$

Figure 3.96 Macrocyclic ligands used to stabilize palladium(III) and platinum(III).

Next Page